Palacký University Olomouc

Master thesis

Olomouc 2023   Bc. Kamila Baslarová

Palacký University Olomouc
Faculty of Science
Department of Cell biology and Genetics

Cytotoxicity of non-taxane microtubule-stabilising drugs in hypoxic cancer cells

Master thesis

Bc. Kamila Baslarová

Study program: Biology

Field of study: Molecular and cell biology

Form of study: Full time

UNIVERZITA PALACKÉHO V OLOMOUCI
Přírodovědecká fakulta
Akademický rok: 2021/2022

ZADÁNÍ DIPLOMOVÉ PRÁCE
(projektu, uměleckého díla, uměleckého výkonu)

Jméno a příjmení:	Bc. Kamila BASLAROVÁ
Osobní číslo:	R21923
Studijní program:	N0511A030046 Molekulární a buněčná biologie
Téma práce:	Cytotoxicita netaxanových mikrotubuly stabilizujících léčiv v hypoxických rakovinných buňkách
Zadávající katedra:	Katedra buněčné biologie a genetiky

Zásady pro vypracování

Microtubule-stabilising drugs like the taxanes are critical adjuvant and palliative therapies for the treatment of metastatic solid tumours of different lineages. However, tumour hypoxia-mediated changes are one of the major contributors to the development of taxane resistance. This thesis will characterise the effects of non-taxane microtubule-stabilising drugs in hypoxic cancer cells for potential development as antitumor agents.

Rozsah pracovní zprávy:
Rozsah grafických prací:
Forma zpracování diplomové práce: tištěná
Jazyk zpracování: Angličtina

Seznam doporučené literatury:

CHEN, Guanglin, Ziran JIANG, Qiang ZHANG, Guangdi WANG a Qiao-Hong CHEN. New Zampanolide Mimics: Design, Synthesis, and Antiproliferative Evaluation. *Molecules* [online]. 2020, 25(2) [cit. 2021-10-26]. ISSN 1420-3049. DOI:10.3390/molecules25020362

DAS, Viswanath, Francesca BRUZZESE, Petr KONEČNÝ, Federica IANNELLI, Alfredo BUDILLON a Marián HAJDÚCH. Pathophysiologically relevant in vitro tumor models for drug screening. *Drug Discovery Today* [online]. 2015, 20(7), 848-855 [cit. 2021-10-26]. ISSN 13596446. DOI:10.1016/j.drudis.2015.04.004

DAS, Viswanath, Jana ŠTĚPÁNKOVÁ, Marián HAJDÚCH a John H. MILLER. Role of tumor hypoxia in acquisition of resistance to microtubule-stabilizing drugs. *Biochimica et Biophysica Acta (BBA) – Reviews on Cancer* [online]. 2015, 1855(2), 172-182 [cit. 2021-10-26]. ISSN 0304419X. DOI:10.1016/j.bbcan.2015.02.001

FIELD, Jessica, Peter NORTHCOTE, Ian PATERSON, Karl-Heinz ALTMANN, J. DÍAZ a John MILLER. Zampanolide, a Microtubule-Stabilizing Agent, Is Active in Resistant Cancer Cells and Inhibits Cell Migration. *International Journal of Molecular Sciences* [online]. 2017, 18(5) [cit. 2021-10-26]. ISSN 1422-0067. DOI:10.3390/ijms18050971

GHOSH, Arun K. a Xu CHENG. Enantioselective Total Synthesis of (−)-Zampanolide, a Potent Microtubule-Stabilizing Agent. *Organic Letters* [online]. 2011, 13(15), 4108-4111 [cit. 2021-10-26]. ISSN 1523-7060. DOI:10.1021/ol201626h

PERONNE, Lauralie, Eric DENARIER, Ankit RAI, et al. Two Antagonistic Microtubule Targeting Drugs Act Synergistically to Kill Cancer Cells. *Cancers* [online]. 2020, 12(8) [cit. 2021-10-26]. ISSN 2072-6694. DOI:10.3390/cancers12082196

ŘEHULKA, Jiří, Narendran ANNADURAI, Ivo FRYDRYCH, et al. Cellular effects of the microtubule-targeting agent peloruside A in hypoxia-conditioned colorectal carcinoma cells. *Biochimica et Biophysica Acta (BBA) – General Subjects* [online]. 2017, 1861(7), 1833-1843 [cit. 2021-10-26]. ISSN 03044165. DOI:10.1016/j.bbagen.2017.03.023

ŘEHULKA, Jiří, Narendran ANNADURAI, Ivo FRYDRYCH, Petr DŽUBÁK, John H. MILLER, Marián HAJDÚCH a Viswanath DAS. Peloruside A-Induced Cell Death in Hypoxia Is p53 Dependent in HCT116 Colorectal Cancer Cells. *Journal of Natural Products* [online]. 2018, 81(3), 634-640 [cit. 2021-10-26]. ISSN 0163-3864. DOI:10.1021/acs.jnatprod.7b00961

Vedoucí diplomové práce: Mgr. Viswanath Das, PhD.
                             Ústav molekulární a translační medicíny

Datum zadání diplomové práce: 29. října 2021
Termín odevzdání diplomové práce: 31. července 2023

doc. RNDr. Martin Kubala, Ph.D.   prof. RNDr. Zdeněk Dvořák, DrSc.
            děkan   vedoucí katedry

V Olomouci dne 11. listopadu 2021

BIBLIOGRAPHICAL IDENTIFICATION

Author's name	Bc. Kamila Baslarová
Title	Cytotoxicity of non-taxane microtubule stabilising drugs in hypoxic cancer cells
Type of thesis	Master
Department	Cell Biology and Genetics, Faculty of Science UP, Olomouc
Supervisor	Mgr. Viswanath Das, Ph.D.
The year of defense	2023

Summary

Microtubule targeting agents like paclitaxel or vinblastine, usually originating in nature, are frequently used in the chemotherapy of solid tumors. Their binding to microtubules distorts microtubule dynamics, cellular transport, and mitosis. However, these therapeutics are susceptible to elimination via drug resistance mechanisms developed in targeted cells. The development of resistance mechanisms may be enhanced by the hypoxic microenvironment inside solid tumors. The cells' response to hypoxia is mediated by a transcription factor HIF-1α, which targets genes for anti-apoptotic proteins, drug efflux pumps, enzymes of glucose metabolism, and others. Zampanolide is a novel non-taxane microtubule-stabilizing agent, which binds covalently to the taxane microtubule binding site. This cytostatic may have the potential to avoid some of the resistance mechanisms listed above and affect cells adapted to the hypoxic environment. This thesis evaluated Zampanolide effects on HCT116 human colorectal carcinoma cells. However, a hypoxic environment was able to hinder Zampanolide effects on cells in the experiments used in this study.

Keywords	MSA, Zampanolide, hypoxia, cytotoxicity
Number of pages	66
Number of appendices	0
Language	English

BIBLIOGRAFICKÉ ÚDAJE

Jméno autora	Bc. Kamila Baslarová
Název práce	Cytotoxicita netaxanových mikrotubuly stabilizujících léčiv v hypoxických rakovinných buňkách
Typ práce	Diplomová
Pracoviště	Katedra buněčné biologie a genetiky, PřF UP v Olomouci
Vedoucí práce	Mgr. Viswanath Das, Ph.D.
Rok obhajoby práce	2023

Souhrn

Léčiva cílená na mikrotubuly jako paclitaxel nebo vinblastin, obvykle látky přírodního původu, jsou často užívána jako chemoterapie solidních tumorů. Jejich vazba na mikrotubuly narušuje dynamiku mikrotubulů a tedy intracelulární transport a mitózu. Jsou ale náchylná na eliminaci mechanismy lékové rezistence vzniklými v cílových buňkách. Rozvoj lékové rezistence může být posílen hypoxickým mikroprostředím uvnitř pevných nádorů. Odpověď buněk na hypoxii je zprostředkovávána transkripčním faktorem HIF-1α, jenž cílí také na geny pro anti-apoptotické proteiny, effluxní pumpy, enzymy metabolismu glukozy a další. Zampanolide je nová netaxanová mikrotubuly stabilizující molekula, které se kovalentně váže do taxanového místa. Může být potenciálně odolná proti mechanismům lékové rezistence vyjmenovaným výše a účinkovat na buňky adaptované na hypoxické prostředí. Tato závěrečná práce evaluovala účinky Zampanolidu na lidskou nádorovou linii kolorektálního karcinomu HCT116. Ovšem v použitých experimentech byla hypoxie schopna negativně ovlivnit efekt Zampanolidu na buňky.

Klíčová slova	MSA, Zampanolid, hypoxie, cytotoxicita
Počet stran	66
Počet příloh	0
Jazyk	Anglický

DECLARATION

I declare, that this master thesis was written independently with help of my supervisor Mgr. Viswanath Das, Ph.D., and using the sources listed in the references.

In Olomouc, ………………………

………………………

Kamila Baslarová

ACKNOWLEDGEMENT

CONTENTS

ABBREVIATIONS

AhR	Aryl hydrocarbon receptor
AKT	Protein kinase B
ARF	Alternate reading frame protein
ARNT	Aryl hydrocarbon receptor nuclear translocator
ATM	Ataxia-telangiectasia mutated kinase
ATR	Ataxia telangiectasia and Rad3-related protein
Bcl-2	B-cell lymphoma 2 protein family (Bak, Bax, Bid)
CAIX	Carbonic anhydrase IX
CBP	CREB binding protein
CHK	Checkpoint kinase
CREB	cAMP response element-binding protein
Erg 1	Early growth response 1 transcription factor
ERK	Extracellular signal-regulated kinase
FDA	Food and Drug Administration
FIH-1	Factor Inhibiting HIF-1
HIF-1	Hypoxia-inducible factor 1
HRE	Hypoxia-responsive elements
LAU	Laulimalide
MAPs	Microtubule associated proteins
MAPK	Mitogen-activated protein kinase
MDA	Microtubule destabilizing agent
MDM2	Mouse double minute 2 homolog
MDR1	Multidrug resistance 1 gene
NF-κB	Nuclear factor kappa-light-chain-enhancer of activated B cells
MSA	Microtubule stabilizing agent
MTA	Microtubule targeting agent
mTOR	Mammalian target of rapamycin
PARP	Poly (ADP-ribose) polymerase

PHDs	Prolyl hydroxylase domain proteins
PDGF	Platelet-derived growth factors
PI3K	Phosphoinositide3-kinase
PKC	Protein kinase C
PLA	Peloruside
PLCγ	Phospholipase Cγ
PTX	Paclitaxel
Raf	Rapidly Accelerated Fibrosarcoma serine/threonine kinase
Ras	Rat sarcoma virus – small GTPase
VBL	Vinblastine
VEGF	Vascular Endothelial Growth Factor
VHL	Von Hippel Lindau tumor suppressor
YC-1	3-(5′-hydroxymethyl-2′-furyl)-1-benzylindazole
ZAMP	Zampanolide

LIST OF FIGURES

LIST OF GRAPHS

LIST OF TABLES

1 INTRODUCTION

Microtubule targeting agents like paclitaxel or vinblastine, usually originating in nature are frequently used in the chemotherapy of solid tumors. They cause either stabilization or destabilization of microtubules. The consequences of disruption of microtubule dynamics cause distortions in cellular transport and mitosis, leading to apoptosis mainly in populations of fast-dividing cancer cells. Their potential could be hindered by the development of multidrug resistance phenotypes in cancer cells, which can emerge as a byproduct of the hypoxic conditions inside the solid tumor microenvironment. For example, taxanes, originating from *Taxus brevifolia*, are susceptible to elimination by the drug efflux pump P-gp. Changes in intracellular pH caused by alternated glucose metabolism and expression of β-tubulin isotypes can also contribute to taxane resistance.

The response to hypoxia in cells is mediated by a transcription factor HIF-1α. Target genes of HIF-1α include anti-apoptotic proteins, drug efflux pumps, enzymes of glucose metabolism, and others.

Zampanolide is a new non-taxane microtubule stabilizing agent, which has the potential to avoid some of the resistance mechanisms listed above due to its covalent bonding to its binding site.

The aim of this thesis was to investigate Zampanolide's potential in inhibiting the growth of human colorectal HCT116 carcinoma cells *in vitro* and to determine if alterations in levels of HIF-1α and p53 modulate the cytostatic effects of Zampanolide.

2 AIM OF THE THESIS

Determine the effects of Zampanolide on human colorectal carcinoma cell line HCT116 in hypoxic and normoxic conditions.

OBJECTIONS

1. Determine and compare IC_{50} values of Zampanolide and YC-1 in HCT116 parental cell line, HCT116 p53 knockout cell line, and hypoxia reporter cell line (HCT116 HIF-1α) in normoxic and hypoxic conditions. YC-1 was used as a positive anti-HIF-1α inhibitor.

2. Report the effect of Zampanolide on tubulin polymerization in HCT116 parental cells, HCT116 p53 knockout cells, and hypoxia reporter cell line (HCT116-HIF-1α) in normoxic and hypoxic conditions.

3. Determine if Zampanolide-induced apoptosis is Caspase 3 and 8, or PARP dependent.

4. Conclude if Zampanolide effects are p53 and HIF-1α dependent and if they are influenced by hypoxia.

3 LITERATURE REVIEW

3.1 HYPOXIA

Oxygen levels in Earth's atmosphere rose dramatically 2.4–2.0 billion years ago due to the expansion of cyanobacteria, which generated O_2 as a waste side product of their metabolism. And though the exact causes and mechanisms of this 'Great Oxidation Event' are still a subject of academic debate, the major consequences are clear (Lyons et al., 2014).

Nowadays, our planet is inhabited by many aerobic organisms that use oxygen to oxidize complex biomacromolecules to CO_2. Through this process, the organisms utilize the energy of macroergic bonds of the substrate to produce adenosine triphosphate (ATP) and other macroergic compounds that can serve as a universal energy source in synthesis pathways of cells, cytoskeletal movement, homeostasis maintenance, etc. (Alberts et al., 2008).

Therefore, the abundance of oxygen is crucial for proper cell function, and its absence is a significant stressor. Cell needs to arrest pathways that are not essential for survival. Cells need to preserve energy in the form of ATP because reactions like aerobic respiration and fatty acid desaturation, which lead to ATP production, are O_2 dependent (Alberts et al., 2008).

Cell's response to hypoxia is mediated by a transcription factor known as hypoxia-inducible factor 1 (HIF-1), which consists of two subunits, HIF-1α and HIF-1β. HIF-1α was identified by Gregg Semenza (Nobel Prize 2019). HIF-1β is also known as the aryl hydrocarbon receptor nuclear translocator (ARNT), and it is also a dimerization partner for the Aryl hydrocarbon receptor (AhR). HIF-1β is expressed constitutively, whereas HIF-1α levels are regulated by the presence of O_2.

In normoxia, HIF-1α is polyubiquitinated and destroyed by proteasome machinery. The process of HIF-1α oxygen-dependent regulation is illustrated in Figure 3.1. The signaling cascade starts with dioxygenases known as prolyl hydroxylase domain proteins (PHDs) that serve as oxygen sensors because they utilize oxygen as a cosubstrate. Fe^{2+} and α-ketoglutarate are also needed for PHD's activity as cofactors. PHD's function is to hydroxylate two proline residues of HIF-1α located on the O2-dependent degradation (ODD) domain, while the α-ketoglutarate is decarboxylated to succinate. Hydroxylated HIF-1α is recognized by the von-Hippel Lindau tumor suppressor (pVHL), which is part of the VHL protein complex with elongin B and C, and cullin-2 (E3 ubiquitin ligase complex). HIF-1α is then polyubiquitinated and destroyed (Lee et al., 2020) (Das et al., 2015).

HIF-1α activity is also controlled by HIF asparaginyl hydroxylase or FIH-1 (Factor Inhibiting HIF-1), which is also dioxygenase. However, FIH-1 hydroxylates the C-terminal

transactivating domain of HIF-1α on asparaginyl residue when the oxygen is present to enable HIF-1α interaction with transcription coactivators E1A binding protein p300 (P300) and CREB-binding protein (CBP) (Lee et al., 2020) (Das et al., 2015).

When oxygen levels in the tissue are below 5 %, and HIF-1α is not destroyed, HIF-1α forms a dimer with ARNT and binds to hypoxia-responsive elements (HRE) in the nucleus. HIF-1, for example, modulates glucose metabolism by binding into the promoters of genes encoding glucose transporters (GLUT1 and GLUT3) and enzymes of the glycolytic pathway like phosphofructokinase-liver type, aldolase, phosphoglycerate kinase-1, enolase, and lactate dehydrogenase-A, increasing their expression, since the ATP cannot be sourced from the respiratory chain and Krebs cycle due to lack of oxygen. (Semenza et al., 1994).

Another critical target of HIF-1 is the Vascular Endothelial Growth Factor (VEGF-A) gene. VEGF-A is crucial in angiogenesis, which occurs during embryonal development, after injury, or during solid tumor growth. This mechanism will be described in the following chapter.
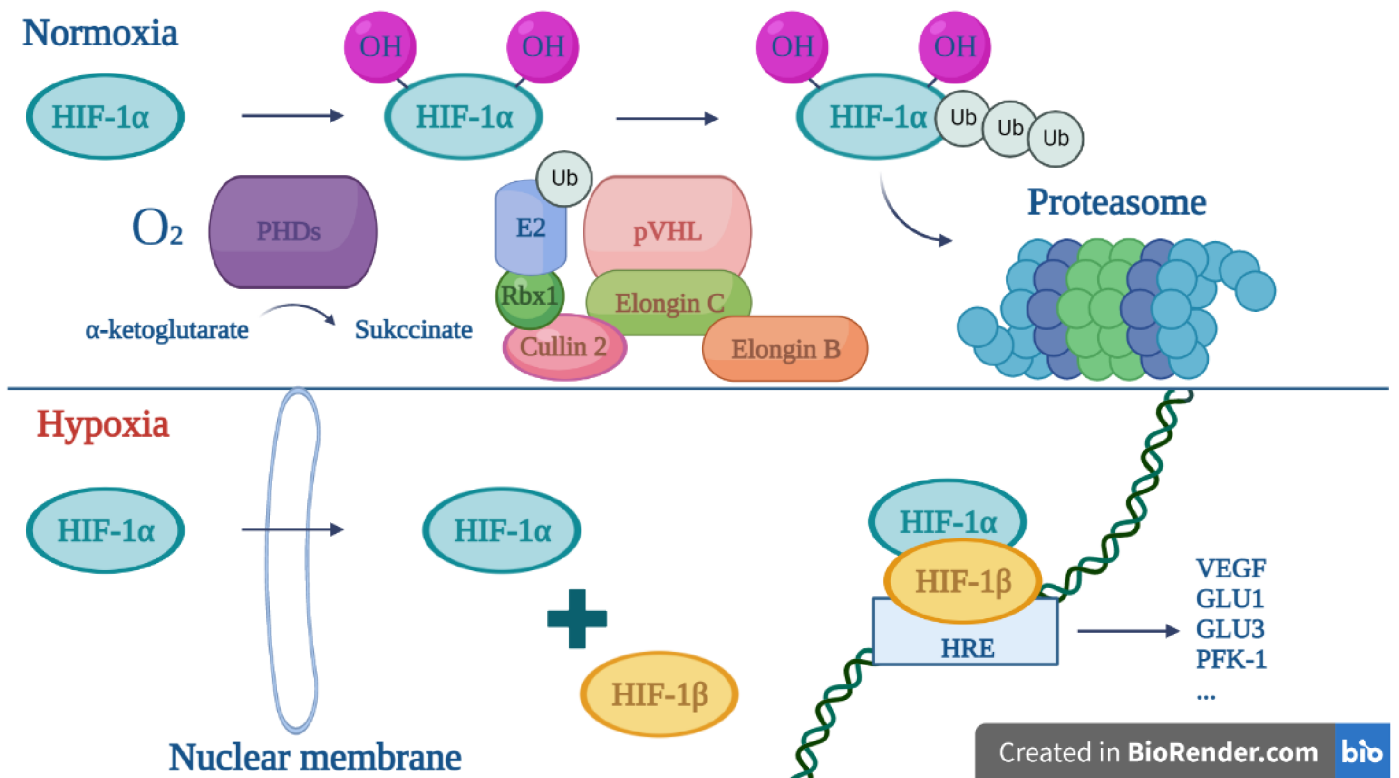
Figure 3.1 – HIF-1α signaling in normoxia and hypoxia. In the presence of oxygen, HIF-1α is hydroxylated by PHDs and then tagged for proteasomal destruction by pVHL. In the absence of oxygen, HIF-1α dimerizes with HIF-1β and translocates to the nucleus to induce the transcription of target genes in HRE. **Created in BioRender.com**

3.2 HYPOXIA IN CANCER

Cancer is a group of diseases caused by uncontrollable proliferation and spreading of the cells with accumulated mutations in genes that control the cell cycle. According to World Health Organisation, cancer was responsible for approximately 10 million deaths worldwide in 2020. That means every sixth death was caused by cancer. Colorectal cancer is the third most commonly diagnosed cancer globally, which caused one million casualties in 2020. The only cancer type that caused more deaths in 2020 was lung cancer (Hu et al., 2016) (Sung 2021) (WHO 2022).

The development of a tumor is a process of microevolution during which the cells accumulate somatic mutations. If cells divide and form a mass, however, they do not have the properties to invade neighboring tissue and spread into distant parts of the body via the bloodstream, the mass is classified as a benign tumor. A tumor with invasive properties that can form metastasis is malignant. The tumors originating in epithelial tissue are carcinomas, and those in mesenchymal tissue are sarcomas. Leukemias are tumors developed from blood-forming tissues; hence they form liquid tumors. That means that abnormal cells originating in the bone marrow are circulating in the bloodstream. Sarcomas and carcinomas are the most common types of solid tumors. They form a mass in the tissue of origin before reaching the bloodstream and metastasizing. These tumor types can sometimes be treated surgically (Alberts et al. 2008)

When solid tumors grow over a diameter of approximately 1 mm, their oxygen demand often exceeds the supply from preexisting blood vessels. The HIF signaling pathway is triggered, and tumor cells express VEGF-A. VEGF-A production results in the development of new blood vessels and, therefore, blood supply for the growing tumor mass. VEGF-A cytokine is a member of the larger family of platelet-derived growth factors (PDGF). After VEGF-A is released, it binds to two targets – VEGF receptors 1 and 2, transmembrane tyrosine kinase receptors on vascular endothelial cells. VEGF-1 receptor is also in monocytes, dendritic cells, and trophoblast cells (Carmeliet 2005).

VEGF-A binding is followed by receptor dimerization and autophosphorylation. The signal is then transducted to downstream signal mediators. This process is well understood in VEGF receptor 2, which transduces the signals via the PLCγ-PKC-MAPK pathway leading to the proliferation of endothelial cells. The kinase activity of VEGF receptor 1 is weaker than the activity of VEGF receptor 2. VEGF-1 knock-out mice embryos develop lethal abnormalities like thicker endocardial lining of their hearts and thick fused blood vessels

with a localized groups of endothelial cells. Thus, it is suspected that the VEGF receptor 1 plays a crucial role in the negative regulation of vascularization in the embryonic stage of development (Fong et al., 1995) (Shibuya et al., 2012). However, studies in human breast cancer xenografted mice suggested that when VEGF receptor 1 is blocked with a monoclonal antibody, depletion of its signaling increases tumor apoptosis. These results align with the hypothesis that VEGF receptor 1 signaling also promotes vascularization and tumor proliferation (Carmeliet 2005) (Wu et al., 2006).

For the reasons listed above, vascularization is one of the targets for cancer treatment. Several angiogenesis inhibitors are on the market right now, including monoclonal antibodies binding to VEGF-A (Bevacizumab) as well as inhibitors targeting the whole spectrum of VEGF receptors (Cabozantinib, Axitinib) (Stukalin et al., 2016). Nonetheless, vascularization is a downstream effect of HIF-1α signaling. HIF-1α is also overexpressed in 50 % of solid tumors and its levels correlate negatively with patients' prognosis. Therefore, HIF-1α is a potential target molecule for antiangiogenesis therapy (Das et al., 2015).

One of the small molecules that can interfere with HIF-1α levels is 3-(5′-hydroxymethyl-2′-furyl)-1-benzylindazole (YC-1). In hypoxia, the mouse retinal tumor 661W cells treated with YC-1 had lowered levels of HIF-1α, while the levels of p53 were increased. The proliferation of cells decreased due to cycle cell arrest and elevated levels of apoptosis. However, the levels of HIF-1α mRNA remained unchanged, including HIF-1α protein half-life. YC-1 effects on HIF-1α protein levels are the consequences of suppression of the PI3K/Akt/mTOR pathway, which stimulates HIF-1α translation, and it is briefly discussed in the following chapter (Tsui et al., 2013) (Sun et al., 2007).

3.4 HYPOXIA AND DRUG RESISTANCE

Hypoxia not only affects tumor vascularization but also contributes to various mechanisms of drug resistance in cancer therapy. The mechanisms of resistance development are sometimes present even in normoxia and are dependent on the cell type. However, hypoxia can contribute to their severity.

Conversely, some cells may activate the expression of HIF-1α independently of the hypoxic conditions via an alternative signaling pathway. This effect was noted in melanoma cells, capable of triggering HIF-1α expression via the Ras/Raf/MAPK(MEK)/ERK pathway. About 20 % of melanoma cells have a mutation in the N-Ras oncogene. These mutations can make N-Ras constitutively active. Its downstream effector is a serine/threonine kinase RAF, which has three isoforms, one of which is BRAF. Mutations in BRAF, which lead to its elevated activity, are also commonly present in melanoma cell lines. The Ras/Raf/MAPK(MEK)/ERK pathway signaling results in HIF-1α expression. The extracellular signal-regulated kinase (ERK) also phosphorylates and uprelugates the HIF-1α coactivator CBP/p300 (Malekan et al., 2021).

HIF-1α transcription may also be activated via the PI3K/Akt pathway induced by the N-Ras oncogene or a tyrosin-kinase receptor signal. When PI3K is activated, it interacts with the PIP2 in the cell membrane, leading to PIP2 phosphorylation to PIP3. PIP3 can activate Akt and, therefore, mTOR. A downstream effector of mTOR is S6K, which binds to ribosomes to stimulate HIF-1α transcription, while the HIF-1α mRNA levels remain unchanged (Mills et al., 2009) (Vu and Aplin, 2016) (Zhang et al., 2018). The alternative pathways that lead to upregulated translation of HIF-1α are illusrated in Figure 3.2.
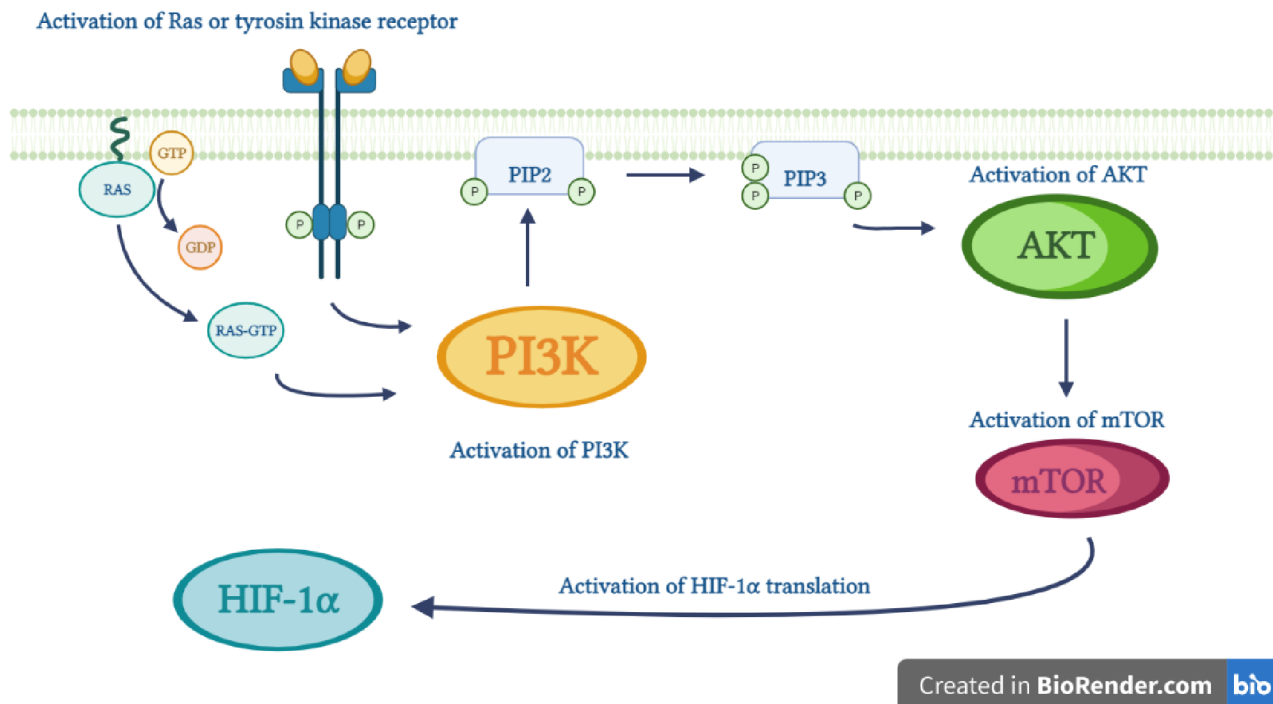
Figure 3.2 – The process of upregulation of HIF-1α transcription via Ras/PI3K/Akt/mTOR pathway. PI3K kinase can be activated via signals from tyrosine kinase receptors or through Ras. It phosphorylates PIP2 to PIP3, which activates AKT kinase and, therefore, mTOR and HIF-1α translation. **Created in BioRender.com**

3.4.1 P-gp overexpression

One of the strategies that cells use to evade the effects of chemotherapy is overexpression of drug efflux pumps from the ATP-binding cassette transporter family like P-gp, a product of the MDR1 gene. P-gp has two ATP binding sites and 12 transmembrane domains. It can bind hydrophobic substrates with positive or neutral charge directly from the cell's cytoplasmatic membrane via its transmembrane domains. A second ATP hydrolysis is required to restore the conformation modifications of the transporter after the substrate has been delivered into the cytoplasm or extracellular space following ATP hydrolysis. P-gp has a large number of substrates, including microtubule-destabilizing agents (MDAs) and microtubule-stabilizing agents (MSAs), such as paclitaxel and docetaxel (Gottesman et al. 2002).

According to some studies, HIF-1α signaling may be connected to MDR1 overexpression because the promotor of the MDR1 gene contains functional HRE (Comerford et al. 2002).

3.4.2 Expression of antiapoptotic proteins

Another mechanism by which hypoxia contributes to drug resistance is the expression of antiapoptotic proteins, like Bcl-2, Bcl-XL, and survivin. Apoptosis may be induced via extracellular signaling pathways and cell death receptors or intracellular pathways due to mitochondrial membrane permeabilization, which enables the spill of small molecules like cytochrome C into cytoplasm and activation of caspases. The mitochondria permeabilization depends on proteins from the Bcl-2 family. Some of those proteins have pro-apoptotic effects, like Bax and Bak and can form channels in the mitochondria membrane and others, like Bcl-2, Bcl-XL inhibits the formation of the channels by blocking Bax and Bak translocation. Also, the expression of pro-apoptotic proteins Bax, Bak, and Bid is downregulated in hypoxia. On the other hand, these changes in expression can occur independently of HIF-1 signaling. The effects of hypoxia on apoptosis also depend on the cell type (Das et al., 2015) (Kim et al., 2005).

In the case of survivin, the overexpression of HIF-1α directly correlates with the overexpression of this protein and higher survivin levels are associated with a poorer prognosis in patients. The promotor of survivin encoding gene BIRC5 contains HRE. Survivin inactivates caspase 3 and 9. Caspase 9 is a key regulator of the apoptosis pathway, and it is activated due to mitochondria membrane permeabilization. Caspase 3 is one of the executive caspases that degrade cytoskeletal and nuclear laminar proteins. (Kesavardhana et al.,2020). However, the upregulation of survivin expression can occur independently of hypoxic conditions since HIF-1α expression may be upregulated via PI3K/AKT pathway, even in normoxia (Das et al., 2015).

3.4.3 Changes in intracellular pH

As was established earlier, HIF-1α signaling is responsible for the overexpression of enzymes of glycolysis, which is only natural, because glycolysis is the primary energy source for cells in an environment depleted of oxygen. This change in cells' metabolism is called the Warburg effect, and the consequences are that the acidic byproducts of glycolysis accumulate in the cells. Cells produce a transmembrane enzyme known as carbonic anhydrase IX (CAIX) to maintain homeostasis. Its purpose is to catalyze CO_2 to bicarbonate and proton.

Unfortunately, this leads to pH changes both in intracellular and extracellular environments, which are not beneficial to patients' prognosis since higher intracellular pH contributes to proliferation. Lower extracellular pH is suitable for metastasis and causes resistance to weakly basic anticancer agents. P-gp activity may also be affected by the extracellular pH. It is upregulated if the extracellular space is acidic (Das et al., 2015).

3.4.4 Changes in tubulin isotype expression

Cancer cells also have strategies to evade the effects of microtubule-targeting agents (MTAs). The mechanisms of actions of MTAs will be explained in detail in the next chapter. The binding of MTAs to tubulin may be affected via the expression of different tubulin isotypes. The TUBB3 β-tubulin overexpression is associated with poorer treatment outcomes in patients with gastric cancers (Yu et al., 2014). At least one study suggested that the TUBB3 expression may be influenced by HIF-1α. The experiments showed that the hypoxia-induced expression of TUBB3 made the tubulin isolated from the A2780 human ovarian cancer cells resistant to polymerization after in vitro treatment by paclitaxel. Moreover, this effect can be reversed after interference with HIF-1α. In the same study, TUBB3 levels dropped after the knockdown of HIF-1α via RNA interference (Raspaglio et al., 2008).

In hypoxia, microtubules can also be protected from the destabilizing effects of microtubule-destabilizing agents (MDAs), like nocodazole and vinblastine. The stabilization of the microtubules is induced via early-growth response 1 (Erg-1) protein, which serves as a transcription factor, and whose transcription is elevated in hypoxia. After activation, Erg-1 translocates into the cell nucleus to enhance the transcription of its target genes. However, a part of the Erg-1 population remains in the cytoplasm colocalized with microtubules and protected them from MDAs-induced destabilization. The protective effects of Erg-1 on microtubules were observed in the BEL-7402 cell line. After the knockdown of Erg-1 via RNA interference, the protective effects of hypoxia decreased (Peng et al., 2010).

3.4.5 p53 in hypoxia

Hypoxia may also affect the activity of the tumor suppressor gene p53. Mutations in the p53 gene are present in 50 % of human cancers, and p53 null mice are prone to develop neoplasms before 6 months of age. Although the study cited included only 35 mice homozygous for the p53 disrupted allele, 26 of the animals developed some neoplasms, sometimes as early as 0 weeks of age (Donehower et al., 1992).

11

The p53 protein is a transcription factor that can be expressed as at least 12 different isotypes depending on the tissue of origin. In cells unaffected by stress, p53 is kept below a significant level by E3 ubiquitin ligase MDM2, which catalyzes p53 ubiquitinylation and proteasome degradation. The MDM2 gene is also a target of p53, which upregulates MDM2 transcription, creating a self-regulating negative feedback loop (Meek 2004). The newly synthesized MDM2 will tag the remaining p53 for degradation after cellular stress like DNA damage is resolved. Various stressors may activate the p53. One of the most important roles of p53 is to arrest cell division and promote DNA repair after DNA damage. The DNA strand breaks will attract proteins responsible for activating kinases, ATR and ATM. These kinases will phosphorylate the downstream kinases CHK2 and CHK1, which will phosphorylate MDM2/MDM4 and p53 complex, thus stabilizing p53. MDM4 is a protein related to MDM2, which enhances the ubiquitinylation activity of MDM2 (Liebl and Hofmann, 2021).

An alternative pathway of p53 activation is a response to the ARF protein, which inactivates MDM2 and thus stabilizes p53. The E2F transcription factors activate the ARF protein expression. Those are downstream targets of mitogen pathways, including Ras oncogene and retinoblastoma tumor suppressor gene (RB) (Sherr and Weber, 2000).

The target genes of p53 are involved in cell cycle arrest, DNA repair, apoptosis, senescence, and autophagy (Liebl and Hofmann, 2021). The details of the p53 regulation are shown in Figure 3.3.
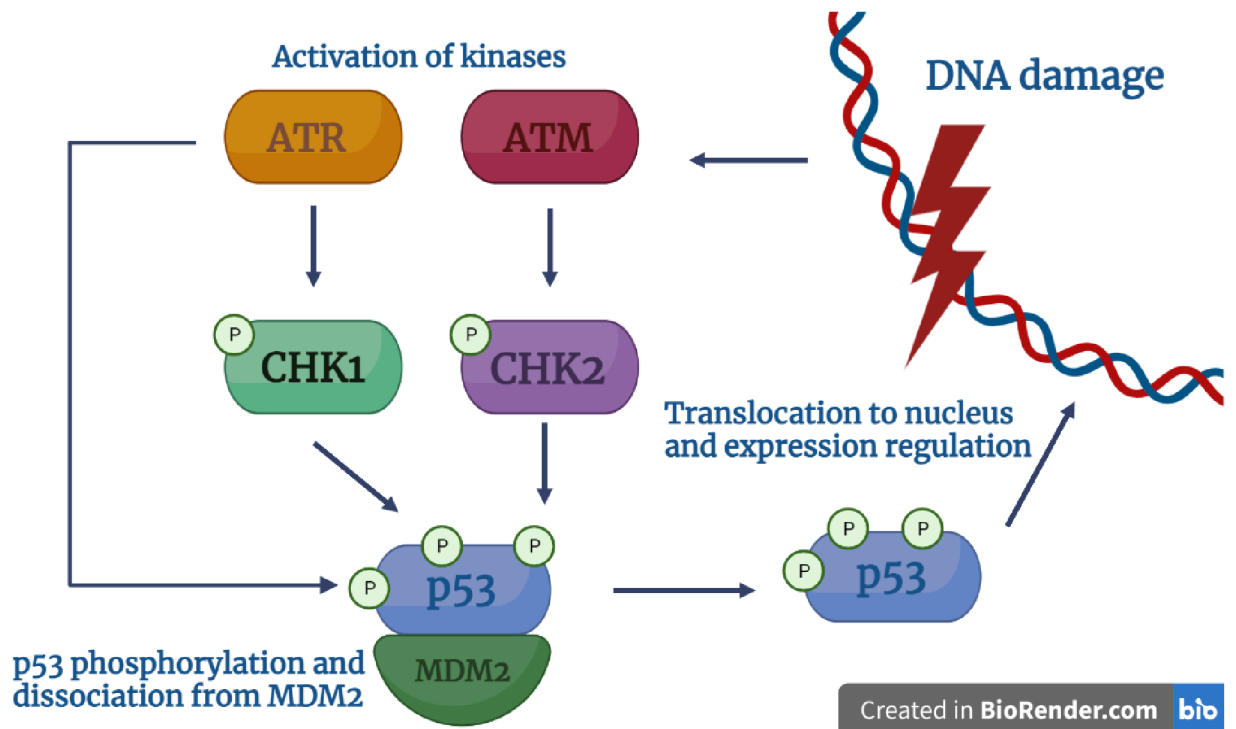
Figure 3.3 – p53 signaling. DNA damage induces the activation of ATR and ATM kinases, which activate downstream kinases CHK1 and 2 or p53 via phosphorylation. p53 translocates into the nucleus to induce the expression of target genes. **Created in BioRender.com**

Mutation in the p53 gene may contribute to the Warburg effect because the reduced activity of p53 lowers the expression of cytochrome c oxidase 2, which is necessary for the respiratory chain function. Also, the absence of functioning p53 leads to the enhancement of glucose transport and metabolism through the NF-κB pathway. Moreover, p53 mutations may contribute to the development of hypoxia-induced drug resistance via CAIX production.

There is significant crosstalk between p53 and HIF-1 signaling pathways because the absence of ATM kinase, which is responsible for p53 activation, may lead to overexpression of both HIF-1 subunits. Also, both HIF-1 and p53 compete for the p300 coactivator (Obacz et al.,2013).

The hypotheses of whether hypoxia causes p53 accumulation or degradation are conflicted. However, Suzuki et al. reported that the relationship between HIF-1α and p53 may be explained by HIF-1α phosphorylation status. If HIF-1α is phosphorylated on the target

residue, it can bind to ARNT and cause the expression of the target gene, promoting cell survival in hypoxia. If HIF-1α is dephosphorylated, it binds to p53 and promotes p53-induced apoptosis (Suzuki et al.,2001).

3.5 MICROTUBULES and MICROTUBULE-TARGETING DRUGS

3.5.1 Microtubule and tubulin characterization, structure, function, and expression

Microtubules are hollow cylindrical protein fibers with an outer diameter of approximately 25 nm and an inner diameter of 16 nm. One microtubule consists of 13 protofilaments. The polymerization of a microtubule usually starts in microtubule organizing centers like centrosomes or basal bodies.

Microtubules are a part of the cellular cytoskeleton, together with microfilaments and intermediate filaments. They play an essential role in the intracellular transport of vesicles and organelles, which can be attached to motor proteins like kinesin and dynein and then transported along the microtubule using the energy of ATP hydrolysis. Microtubules also form the mitotic spindle during the division of the nucleus. They attach to chromosomes via kinetochores to distribute genetic information equally into new daughter nuclei. Both kinetochore-microtubule depolymerization and centromere movement, carried out by interacting various microtubules with others and the cell membrane, are responsible for chromosome separation (Alberts et al., 2008).

The building blocks of microtubules are α-tubulins and β-tubulins, proteins with a molecular mass of around 50 kDa, which are 40 % identical in amino acid sequence. Both α-tubulin and β-tubulin monomers have two β-sheets in their core. One β-sheet consists of four β-strands, and the other β sheet of six. The core is surrounded by 12 α-helices. We distinguish three functional domains on each tubulin monomer. First is the highly conservative N-terminal domain capable of binding nucleotides – GTP and GDP. The nucleotide-binding site of α-tubulin is known as E-site. The β-tubulin nucleotide binding site is the N-site. Second is the intermediate domain. In β-tubulin, the intermediate domain contains a taxol-binding site. Last is the C-terminal domain, which comprises helices H11 and H12. Those helices are localized on the surface of microtubules, and therefore, they may be involved in the binding of microtubule-associated proteins (MAPs) and motor proteins. H11 and H12 are also connected by a loop important for interacting with the next monomer in the protofilament. The C-terminal domain ends with hypervariable residues. Those residues may differ depending on the species from where the tubulins were isolated or depending on the tubulin isotype (Nogales et al., 1998).

Twelve genes encoding α-tubulin and ten encoding β-tubulin are present in the human genome. However, two of the α-tubulin-encoding genes are pseudogenes, meaning they

are not transcribed, and one is a putative gene. Among the ten gene encoding β-tubulin, there is only one pseudogene. (Amargant et al. 2019). Various cell types may express different tubulin isotypes. For example, the TUBB3 β-tubulin isotype associated with chemotherapy resistance is usually expressed in non-cancerous neuronal cells and testicular Sertoli cells (Kavallaris, 2010). The tubulin expression may also vary depending on the developmental state of the organism. For example, human oocytes express specifically β-tubulin isotype B8 (TUBB8). Tubulins also undergo post-translational modifications such as acetylation, tyrosination, phosphorylation, or polyglutamylation (Amargant et al. 2019).

3.5.2 Microtubule assembly and dynamics

Microtubule polymerization usually starts in microtubule-organizing centers made up of rings of γ-tubulin and other proteins from the γ-tubulin complex component proteins superfamily. Microtubules are built up from α-tubulin and β-tubulin dimers, while α-tubulin binds to the γ-tubulin on the minus end of the microtubule. The other end of the microtubule with exposed α β-tubulin units is called the plus end. The α-tubulins and β-tubulins both bind GTP into their nonexchangeable E-site on α-tubulin or exchangeable N-site on β-tubulin. Only the GTP bound to β-tubulins can be hydrolyzed into GDP shortly after polymerization. As the microtubule grows longer and the GTP is continuously hydrolyzed, only the tubulin dimers that were added recently contain GTP bound to β-tubulin. This part of the microtubule is a GTP cap. The presence of GTP has effects on microtubule stability and dynamics. When all the GTP molecules are hydrolyzed to GDP, the microtubule is destabilised and susceptible to rapid depolymerization. Microtubules can assemble and then depolymerize in rapid cycles. This process is called dynamic instability (Alberts et al., 2008) (Cooper and Geoffrey, 2002).

3.5.3 Microtubule-Destabilizing Agents

Microtubules became a target for anticancer therapy because of their crucial role in cell division. The molecules with affinity to microtubules that either destabilize or stabilize them are relatively common in plants and animals, such as marine sponges. These organisms probably synthesize these compounds to protect them from potential consumers or predators.

The first discovered microtubule targeting agents (MTAs) were Vinca alkaloids – vinblastine and vincristine. They were isolated from the periwinkle plant (*Catharanthus roseus*). The Vinca-binding site is localized on the β-tubulin subunit and the binding is reversible. In high concentrations, around 10–100 nM, these alkaloids can destroy the mitotic spindle via microtubule depolymerization. However, even lower concentrations

of these alkaloids can stop mitosis, likely due to changes in microtubule dynamics. In the presence of Vinca alkaloids, the growth and depolymerization rate at the assembly end of the microtubule is slower. The mitotic spindle cannot assemble, and the tension at the kinetochores necessary for cell cycle signaling is reduced. Vinca alkaloids are used to treat testicular carcinoma and Hodgkin and non-Hodgkin lymphomas, breast cancer, and germ cell tumors (Moudi et al., 2013). The side effect of this treatment is peripheral neuropathy, which may be caused by disruption of axonal flow secured by microtubular transport or demyelination. Other side effects include myelosuppression and its consequences since the antimitotic properties of Vinca alkaloids interfere with rapid mitosis in hematopoietic stem cells. (Jordan et Wilson, 2004).

One of the MDAs, colchicine, was used in ancient history to treat joint pain as an herbal remedy prepared from Colchicum autumnale. Colchicine disturbs the structure of the tubulin dimer by binding to the β-tubulin subunit, which causes the straight tubulin dimer to curve, and therefore, the microtubule assembly is prevented (Liu et al., 2012). Although, in theory, colchicine could be used to treat tumors, its potential is hindered by its low therapeutic index. The US FDA has approved Colchicine for treating familial mediterranean fever and acute gout flares because colchicine-induced destabilization of microtubules interferes with proinflammatory pathways involved in gout development (Dalbeth et al., 2014).

3.5.4 Microtubule-Stabilizing Agents

Microtubule dynamics can also be disrupted by microtubule stabilization. One of the compounds that can stabilize microtubules is paclitaxel, a tetracyclic diterpenoid, isolated from *Taxus brevifoliaand*. It binds to polymerized tubulin, not the free tubulin dimers, in the taxoid-site on β-tubulin, accessible from inside the microtubule. This non-covalent bond will affect tubulin conformation so that the tubulin is more susceptible to polymerization. To trigger microtubule polymerization, the stoichiometric binding of paclitaxel is necessary, which means binding one paclitaxel molecule to one β-tubulin taxoid site. However, to alter the dynamics of microtubules, only fewer molecules are needed. This inhibition of proper microtubule dynamics affects the cell's ability to undergo cell division. However, it does not cause microtubule bundling. Paclitaxel treats breast and ovarian, non-small-cell lung cancer, and Kaposi's sarcoma. Moreover, its side effects are similar to the side effects of Vinca alkaloids.

Unfortunately, paclitaxel is a substrate of the P-gp pump, and cells also evade the death induced by paclitaxel via transcription of the β-tubulin isotype TUBBIII (Das et al., 2015)(Jordan et Wilson, 2004).

Other MSAs are macrolides isolated from marine sponges, Laulimalide and Peloruside. The binding site of these compounds is localized on β-tubulin. Laulimalide or Peloruside have synergistic effects when combined with taxol MSAs due to their different target sites. Although Laulimalide can be effective in cancer cell lines, which have shown taxol resistance, its use is complicated by its high toxicity (Negi et al., 2015)(Risinger et al., 2009). Moreover, despite Laulimalide's efficacy in cancer cell lines cultivated in vitro, in vivo studies on xenograft mice models of human breast cancer showed only negligible reductions in tumor growth, which came with a price of severe toxicity and high mortality (Liu et al. 2007). However, Johnson et al. (2007) reported that Laulimalide inhibited human colon cancer cells (HCT 116) tumor growth in xenograft severe combined immunodeficient mice models.

3.5.5 Zampanolide

Zampanolide is also a MSA. It was isolated from a marine sponge *Fasciospongia rimosa* in 1996 and again in 2009 from *Cacospongia mycofijiensis* (Field et al., 2009). Together with Laulimalide and Peloruside, it represents a new class of MSAs since it consists of a macrocyclic lactone ring. This structure is typical for commonly used antibiotics and antimycotics – macrolides (Chen and Kingston, 2014). It is possible to synthesize (-)-Zampanolide in a lab with a 51 % yield (Ghosh and Cheng, 2011). The (-)-Zampanolide enantiomer has significant cytotoxicity with IC_{50} ranging from 2–10 nM in various cell lines. In human HCT116 colorectal carcinoma cells, the IC_{50} value was reported to be 7.2 ± 0.8 nM (Ghosh and Cheng, 2011).

Zampanolide also binds to the taxoid site. However, the bond is covalent and irreversible, unlike paclitaxel, while the Asn228 and His229 β-tubulin residues are permanently alkylated. Zampanolide induces allosteric changes to tubulin structure and causes it to be more prone to polymerization. The result of microtubule stabilization by Zampanolide is G2/M arrest of the cell cycle. Also, Zampanolide is not susceptible to the elimination by the P-gp efflux pump, probably because of the covalent binding to its target site, and the expression of β-tubulin isotypes like TUBBIII does not reduce the binding of Zampanolide. Mutations in the taxane binding site are also known to cause resistance to taxanes in various cell lines; however, Field et al. reported that cell lines resistant

to paclitaxel with single amino acid mutations in β1-tubulin did not develop resistance to Zampanolide. In the same study, authors attempted to cultivate cell lines resistant to Zampanolide. They cultivated human 1A9 ovarian endometrioid adenocarcinoma cells in media with a gradual increase in Zampanolide levels for approximately one year. However, this experiment did not lead to the development of Zampanolide-resistant cells. The cells even became more susceptible to Zampanolide treatment. At the same time, they developed resistance to paclitaxel, which could have been caused by a mutation in the gene for β1-tubulin with an effect on the taxane binding site (Field et al., 2009) (Chen and Kingston, 2014).

Based on these observations, we may suggest that Zampanolide can evade many mechanisms that make cancer cells in hypoxia resistant to chemotherapy like the expression of the P-gp pump, which gene is a target for HIF-1α, mutations in taxoid binding site, and expression of tubulin isotypes. Therefore, the Zampanolide effect on hypoxic cancer cells should be the same or even more profound than the effect on cells in normoxic conditions.
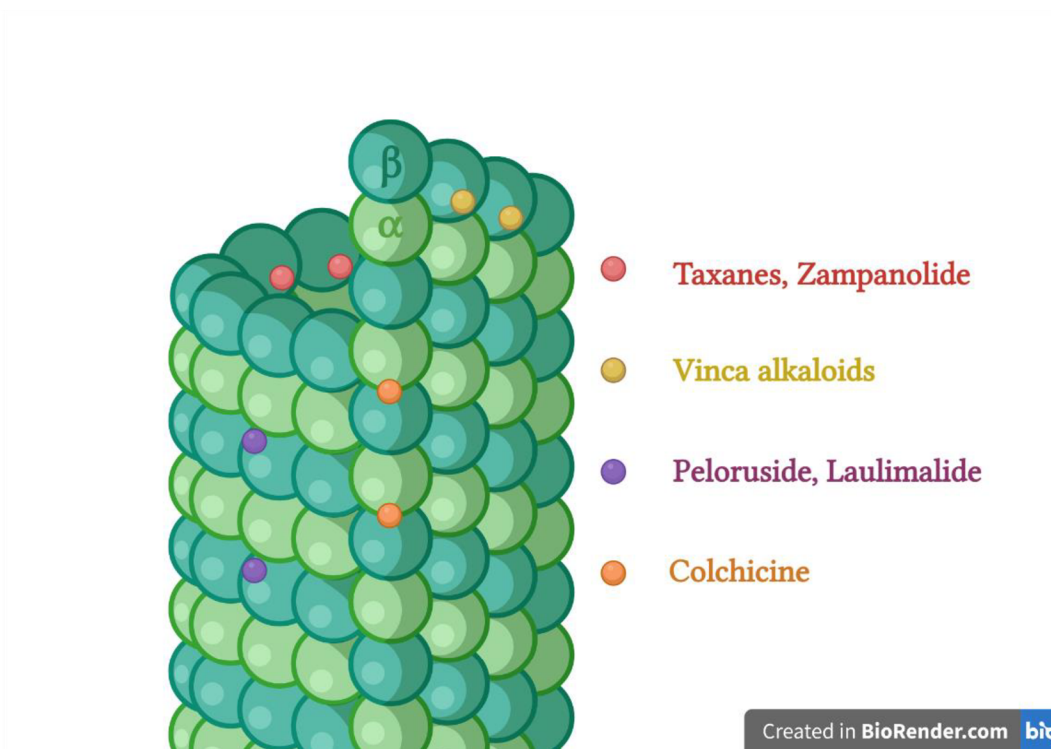

Figure 3.4 – MTAs binding sites. Taxane MTAs and Zampanolide bind to β-tubulin from the inside of the microtubule. Vinca alkaloids bind to β-tubulin subunit at the plus end of the microtubule. Peluroside and Laulimalide bind to β-tubulin from the outside of the microtubule. The colchicine binding site is located on β-tubulin at the interface of the α/β-subunits. **Created with BioRender.com**
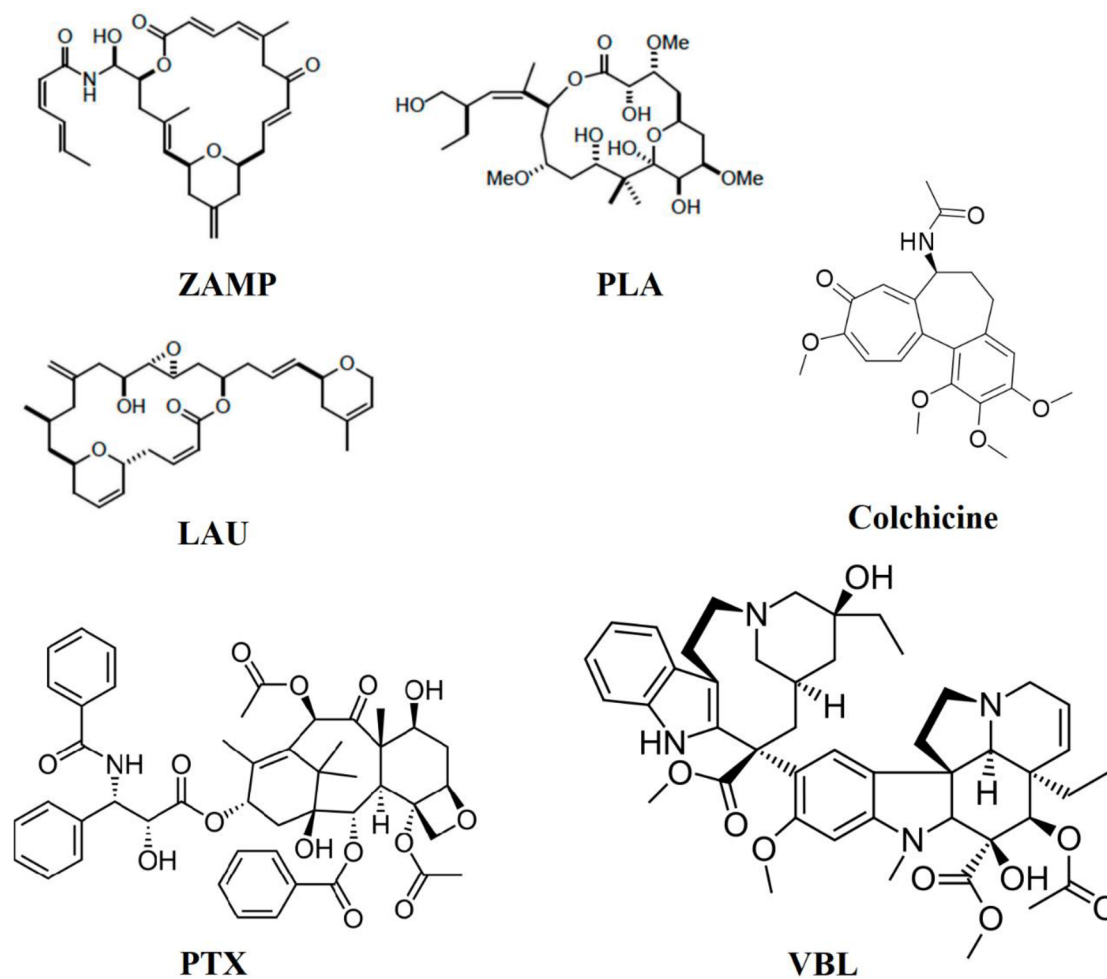
Figure 3.5 – Structure of microtubule targeting agents. ZAMP – Zampanolide. PLA –
Peloruside A, LAU – Laulimalide, Colchicine, PTX – Paclitaxel, VBL – Vinblastine

4 MATERIALS AND METHODS

4.1 Chemicals and reagents

- 2-Mercaptoethanol (Sigma-Aldrich, cat. No. M3148)
- 10x Tris Buffered Saline (TBS) (Bio-Rad, cat. No. 1706435)
- 10x Tris/Glycine/SDS electrophoresis buffer (Bio-Rad, cat. No. 1610772)
- 29% Acrylamide/Bis-acrylamide (Bio-Rad, cat. No. 1610156)
- 98% Ethanol (PENTA, cat. No. 71250-11001)
- Alexa Fluor 488 conjugated goat anti-rabbit IgG secondary antibody (ThermoFisher Scientific™, cat. No. A-11034)
- Alexa Fluor 488 conjugated donkey anti-mouse IgG secondary antibody (ThermoFisher Scientific™, cat. No. A-21202)
- Alpha-Tubulin (α-Tubulin) mouse monoclonal antibody (ThermoFisher Scientific™, cat. No. T5168)
- Bovine serum albumin (BSA) (Sigma-Aldrich, cat. No. A2153)
- Fetal bovine serum (FBS) (Gibco™, cat. No. 10270106)
- Formaldehyde (Fagron, cat No. 614147)
- McCoy's 5A Medium with L-Glutamine (Lonza, cat. No. BE12-688F)
- Methyl alcohol (PENTA, cat. No. 21210-11000)
- PARP rabbit monoclonal antibody (Cell Signaling Technology, cat. No. 9532)
- Protease Inhibitor Cocktail Tablets (Roche, cat. No. 04693116001)
- Phosphatase Inhibitor Cocktail Tablets (Roche, cat. No. 04906837001)
- Resolving gel buffer 1.5 M Tris-HCl; pH 8.8 (Bio-Rad, cat. No. 161-0789)
- Spectra™ Multicolor Broad Range Protein Ladder (ThermoFisher Scientific™, cat. No. 26634)
- Stacking gel buffer 0.5 M Tris-HCl; pH 6.8 (Bio-Rad, cat. No. 161-0799)
- Tetramethylethylenediamine (TEMED) (Bio-Rad, cat. No. 1610801)
- Triton™ X-100, (Sigma Aldrich, cat. No. T-8787-100ML)
- TrypLE™ Express Enzyme 1x, no phenol red (ThermoFisher Scientific™, cat. No. 12604013)
- 2-Mercaptoethanol (Sigma-Aldrich, cat. No. M3148)

4.2 List of solutions

- 0.5% crystal violet solution in 25% methanol

- 8% resolving polyacrylamide gel: 2.6 ml 29% acrylamide/bis-acrylamide, 4.6 ml dH$_2$O, 2.6 ml resolving gel buffer, 100 µl 10% (w/v) SDS, 100 µl 10% (w/v) APS, 10 µl TEMED

- 10x PBS: 80 g NaCl, 2.0 g KCl, 14.4 g Na$_2$HPO$_4$, 2.4 g KH$_2$PO$_4$ dissolved in 800 ml dH$_2$O, pH adjusted to 7.4 with HCl and added dH$_2$O to 1000 ml, sterilized by autoclaving and filtrated

- 10% (w/v) APS: 0.10 g of APS dissolved in 1 ml of dH$_2$O

- 10% (w/v) SDS: 1 g of SDS dissolved in 10 ml of dH$_2$O

- 12% resolving polyacrylamide gel: 4 ml 29% acrylamide/bis-acrylamide, 3.2 ml dH$_2$O, 2.6 ml resolving gel buffer, 100 µl 10% (w/v) SDS, 100 µl 10% (w/v) APS, 10 µl TEMED

- 5x SDS-PAGE loading buffer: 250mmol·l−1 Tris-HCl (pH 6.8), 10% SDS, 30% (w/v) glycerol, 0.5 mol·l−1 DTT, 0.02% (w/v) Bromphenol Blue, 10% Mercaptoethanol

- 5% (w/v) BSA blocking solution: 2,5 g of BSA dissolved in 50 ml of TBST buffer, added TBST to 50 ml

- Hypotonic lysis buffer: 157.6 mg Tris-HCl (10 mmol·l−1, pH 7.9), 74.46 mg EDTA (2 nmol·l−1), 75.56 mg KCl (10 nmol·l−1), 14.28 mg MgCl$_2$ (1.5 nmol·l−1) dissolved in 80 ml of dH$_2$O, pH adjusted to 7.9 with HCl and added dH$_2$O to 100 ml, supplied with 2mmol·l−1 PMSF (20 µl in 1 ml of buffer), protease inhibitors (40 µl in 1 ml of buffer) and phosphatase inhibitor (100 µl in 1 ml of buffer)

- RIPA Lysis and Extraction Buffer (Thermo Scientific™, cat. No. 89901) supplied with 2mmol·l−1 PMSF (20 µl in 1 ml of buffer), protease inhibitors (40 µl in 1 ml of buffer) and phosphatase inhibitor (100 µl in 1 ml of buffer)

- Stacking polyacrylamide gel: 670 µl 29% acrylamide/bis-acrylamide, 2.975 ml dH$_2$O, 1.25 ml stacking gel buffer, 50 µl 10% (w/v) SDS, 50 µl 10% (w/v) APS, 5 µl TEMED

- TBST buffer: 100 ml 1x TBS buffer, 900 ml dH$_2$O, 1 ml 0.1% Tween 20

4.3 Drugs

- YC-1 (Cayman Pharma)
- Zampanolide (provided by Dr Rob Keyzers from the School of Chemical and Physical Sciences, Victoria University of Wellington, Wellington, New Zealand)

4.4 List of equipment

- 6-well, and 96-well plates (TPP Techno Plastic Products AG)
- 12-well plates (Merckmillipore)
- −80 °C freezer (New Brunswick™, Innova®, Eppendorf AG)
- Automatic pipetting filler Pipetus® (Hirschmann™)
- Benchtop Centrifuge 5810R (Eppendorf centrifuge)
- BTD Dry Block Heating System (Grant Instruments™)
- Combined Centrifuge/Vortex mixer Multi-Spin PCV-6000 (Grant-Bio)
- EnSpire Multimode Plate Reader 2300-001M (Perkin Elmer)
- Eppendorf pipettes (0.5–1000 µl)
- FastGene Mini Centrifuge (Nippon Genetics)
- Fume Hood (MERCI)
- HeracellTM VIOS incubator (ThermoFisher Scientific™)
- Laminar flowbox MSC-Advantage™ Class II Biological Safety Cabinet (ThermoFisher Scientific™)
- Molecular Imager® Gel Doc™ XR System (Bio-Rad)
- Olympus IX51 Inverted Phase Contrast Fluorescence Microscope (Olympus)
- pH meter (Denver Instrument)
- PowerPac™ HC Power Supply (Bio-Rad)
- Rotina 420R Centrifuge (Hettich Zentrifugen)
- Trans-Blot Turbo RTA Transfer Kit, PVDF (Bio-Rad, cat. No. 170-4272)
- Trans-Blot Turbo Transfer System (Bio-Rad, cat. No. 1704150)
- ViCell™ XR Cell Viability Analyzer (Beckman Coulter)
- Vortex V-1 Plus (Biosan)

4.5 Biological material

Human colorectal cancer cell lines HCT116 wild type and p53 knockout were purchased from ATCC (Middlesex, U.K.) HCT116-HIF cell line was generated as described elsewhere (Řehulka et al., 2017). All cell lines were maintained in McCoy's 5A media with L-glutamine supplemented with 10% FBS and 1x Penicillin-Streptomycin es. Cells were cultivated in a normoxic incubator with 5% CO_2 at 37 ℃. All experiments requiring hypoxic conditions were performed by placing cells in a humidified incubator with 1% O_2 and 5% CO_2.

4.6 METHODS

4.6.1 Cell culturing and passaging

The cell lines (HCT116 parental cells, HCT116p53 knockout cells, HCT116 HIF-1α cells) were kept in McCoy media and passage every 3–5 days. During passaging, old media was discarded, cells were washed twice with 1x PBS, and TrypLE was added into the culturing flask to detach the cells from the surface. This step required 5 minutes of incubation at 37 °C. Afterwards small amount of media was added into the flask, and the cell suspension was transferred into a centrifuge tube. The suspension was centrifuged at 1500 rpm for 5 minutes. The supernatant was discarded, and the pellet was resuspended in 5 ml of media. Cells were counted using a Vi-CELL analyzer. An appropriate amount of cell suspension was transferred back into the culturing flask with media.

4.6.2 Cell viability assay

Cells were planted into the 96 wells plates in a density 27 000 cells·ml^{-1} for normoxia conditions or 25 000 cells·ml^{-1} for hypoxia conditions. Cells were left to attach overnight in normoxia or hypoxia conditions depending on the experiment setting. The next day the media was removed, and cells were treated using 10 µM YC-1 or 0.5 µM Zampanolide in the first well. Half of the media from the first well was transferred into the second and mixed. This step was repeated to dilute the cytostatics gradually. The treatment continued for 72 hours. Cells were kept either in normoxia or hypoxia incubators. After the treatment, the plates were placed on ice. The cells were washed two times using cold 1x PBS and then stained using 50 µl of crystal violet suspension with 25% methanol. During the staining, which took 20 minutes, the plates were placed on the benchtop rocker. After the staining, the plates were washed with deionized water at least thrice and left to dry. The crystals of the dye were dissolved in 50 µl of methanol. The absorbance was measured on a Microplate Reader. The average blank was subtracted from the absorbance of measured wells. Viability was calculated as the absorbance of the measured well divided by the average absorbance of control wells. GraphPad Prism (GraphPad Software, San Diego, Free trial) was used to create dose-response curves and calculated IC$_{50}$ values.

4.6.3 Tubulin polymerization assay

All three cell lines (HCT116 parental cells, HCT116 p53 knockout cells, HCT116 HIF-1α cells) were planted into 12-well plates at a density of 0.5×10^6 cells·ml^{-1} and left overnight in a normoxia or hypoxia incubator.

The next day the media was removed, and cells were treated with Zampanolide for 24 hours in a normoxia or hypoxia incubator. Used concentrations of Zampanolide were 0, 0.05, 0.1, 0.25, 0.5, and 1 μM. Cells were then washed with 1x PBS and lyzed for 5 minutes at 37 °C by 100 μl of hypotonic buffer, which also contained protease inhibitor (2nm·ml^{-1}), phosphatase inhibitor (2nm·ml^{-1}), and PSMF (2nm·ml^{-1}). The lysates were then collected into Eppendorf tubes, and another 100 μl of supplemented hypotonic buffer was added into the wells to lyse and extract the remaining cells. Lysates were also collected.

The samples were centrifuged at 14 000 rpm for 10 minutes. The supernatant was transferred into a new tube and labelled as unpolymerized tubulin fraction, and the pellet was resuspended in 200 μl of hypotonic buffer and labelled as polymerized tubulin fraction. Isolated proteins were either stored at –80 °C or immediately used for electrophoresis.

Samples for electrophoresis were mixed with loading dye in a 4:1 ratio. The loading dye contained 10 % mercaptoethanol. Samples were boiled for 5 minutes in a dry block set to 95 °C and then loaded into electrophoresis that consisted of stacking gel and 12 % separating gel containing 1 % SDS. A multicolour protein ladder was also loaded next to the samples. Electrophoresis was set at 120 V and run for 90 minutes or until the loading dye reached the end of the gel.

The gels were then loaded into the Trans-Blot Turbo Transfer System, and the proteins were transferred onto PVDF membranes. After the western blotting, the membranes were washed with 1x TBT and blocked by blocking buffer for 1 h on the TubeRoller. After incubation, the membranes were washed four times by 1x TBT and then incubated with primary antibody anti-α tubulin for 1 h or overnight. Membranes were washed four times with 1 x TBT and then incubated with secondary antibody Alexa flour 488 anti-mouse for 1 h in the dark and then finally washed four times with 1x TBT and scanned by Molecular Imager System (BioRad).

Obtained images were processed in ImageJ. The intensity of the background was subtracted from the intensity of the bands. The amount of alfa tubulin in each fraction (polymerized or unpolymerized) was expressed as a percentage of the two fractions combined.

4.6.4 Immunoimaging

Sterilized coverslips were placed inside the six-well plates. Cells were planted onto the top of the coverslip. The density of the cell suspension was 333 000 cells·ml⁻¹, and the used volume varied according to the size of the coverslip. After overnight incubation in the normoxia incubator, the cells were treated with 1 μM Zampanolide and incubated for 1 h in the normoxia or hypoxia incubator.

Media was removed, cells were washed with 1x TBS and then fixed in 10% formalin for 10 minutes. The fixation solution was removed, and cells were washed with 1x TBS. A blocking buffer was added, and slips were incubated for 1 h. Coverslips were washed thrice with 1 x TBS and then covered with primary anti-tubulin antibody dissolved in blocking buffer. Incubation lasted 1 h. The washing was repeated, and a secondary antibody Alexa Fluor 488 anti-mouse was added. After another washing cycle, the cells were stained with DAPI and placed onto the microscope slides. The supervisor obtained the images using a confocal microscope.

4.6.5 Protein isolation and PARP cleavage detection

HCT116 parental cells and HCT116 p53 -/- cells were planted into 6-well plates at a density of 250 000 cells·ml⁻¹ and left to attach overnight in hypoxia. The cells were treated with 0.25x IC_{50}, 0.5x IC_{50}, and 1x IC_{50} of Zampanolide and then placed into hypoxia for 3h, 6h, or 18h. After the treatment, the media was collected into a 15-ml falcon tube, and cells were washed with 1x PBS, which was also collected. Cells were detached from the plates using TrypLE and collected. The tubes were centrifuged at 1500 rpm for 5 minutes. The supernatant was discarded. Cells were resuspended in ice-cold 1x PBS, transferred into the Eppendorf tube, and centrifuged at 2600 rpm for 10 minutes. This step was repeated three times. The pelleted cells were then resuspended in 50 μl of RIPA lysis buffer, and the lysate was sonicated for 1 min (50 % amplitude, 15 sec ON, 15 sec OFF). The samples were centrifuged at 13 000 g for 20 minutes at 4 °C. The supernatant containing proteins was collected and either stored at – 80 °C or processed immediately. The concentration of protein in a sample was determined using a BCA assay. The BCA reagent was prepared by mixing BCA reagent A with BCA reagent B in a 50:1 ratio. Samples were pipetted into 96-well plates alongside the protein standards. 200 μl of BCA reagent was added into each well, and the plate was incubated at 37 °C for 30 minutes. The absorbance was measured with Microplate Reader.

Samples for electrophoresis were mixed with loading dye with 10 % mercaptoethanol in a 4:1 ratio. Samples were boiled for 5 minutes in a dry block at 95 °C and then loaded into electrophoresis that consisted of stacking gel and 8 % separating gel containing 1 % SDS. The electrophoresis was run at 120 V until the separation of the samples. The multicolour protein ladder was run alongside the samples. Separated proteins were transferred onto a PVDF membrane using Trans-Blot Turbo Transfer System. The membrane was incubated in a blocking buffer for 1 h and then with anti-PARP primary antibody overnight at 4 °C. The next day the membrane was washed three times with 1x TBT and then incubated with anti-rabbit Alexa Fluor 488 secondary antibody for 1 h at room temperature. After the incubation, the membrane was washed three times by 1x TBT and then scanned by Molecular Imager System (BioRad).

Obtained images were processed in ImageJ. The intensity of the background was subtracted from the intensity of the bands. The percentage of cleaved PARP was determined as the intensity of the cleaved band divided by the intensity of the uncleaved band.

5 RESULTS

5.1 Zampanolide cytotoxicity

The IC_{50} values of YC-1 and Zampanolide against colorectal cancer cell lines were determined under various culture conditions. The following terms are used in this thesis to define different culture conditions: (1) Condition 1 (Normoxia): The cells are always cultured and treated in normoxia (5% CO2/ atmospheric air); Condition 2 (Hypoxia): Cells are always cultured and treated in hypoxia (5% CO2/1% O2); and Condition 3 (Normoxia→Hypoxia): Cell were cultivated overnight in a normoxia incubator and then moved to a hypoxia incubator after drug treatment.

The results are listed in Table 5.1. The differences between cell responses to YC-1 and Zampanolide treatment are shown in Graphs 5.1–5.5. HCT116 parental, HCT116 p53 -/-, and HCT116-HIF-1α cells were plated in 96-well plates and allowed to attach overnight in a humidified incubator under normoxic conditions. The next day, cells were treated with YC-1 or Zampanolide dose-dependently for 72 h, and the viability of the cells was determined using a crystal violet staining assay. The dose-response curves for all the treated cell lines are captured in Graphs 5.1-5.5.

Table 5.1 – IC_{50} values of YC-1 and Zampanolide in HCT116 cell lines cultivated in various experimental conditions. Mean ± SEM, n = 2–5

Cell line	YC-1 [µM]		
	Normoxia	Hypoxia	Normoxia-Hypoxia
HCT 116 Parental	3.58 ± 0.63	2.9 ± 0.6	-
HCT 116 p53 -/-	-	-	-
HCT 116 HIF1α	2.85 ± 0.31	0.69 ± 0.11	0.28 ± 0.058

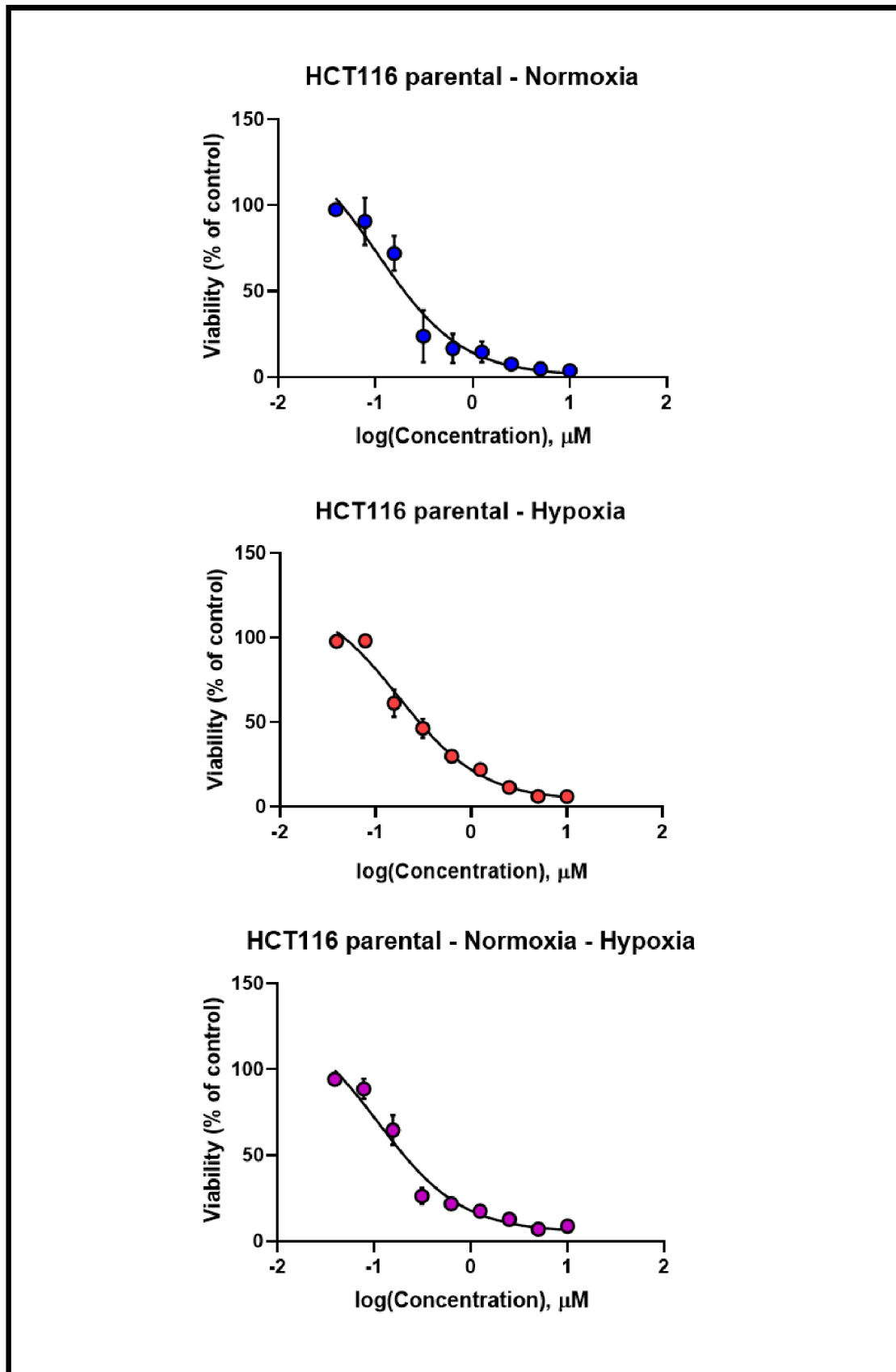|	Zampanolide [µM]		
	Normoxia	Hypoxia	Normoxia-Hypoxia
HCT 116 Parental	0.15 ± 0.04	0.28 ± 0.08	0.1096 ± 0.01
HCT 116 p53 -/-	0.14 ± 0.03	0.38 ± 0.13	0.1392 ± 0.04
HCT 116 HIF1α	0.11 ± 0.02	0.15 ± 0.002	0.2426 ± 0.03

Graph 5.1 – Dose-response curves of YC-1 in HCT116 parental cells cultured in normoxia and hypoxia. Data are presented as mean ± SEM, n = 3.
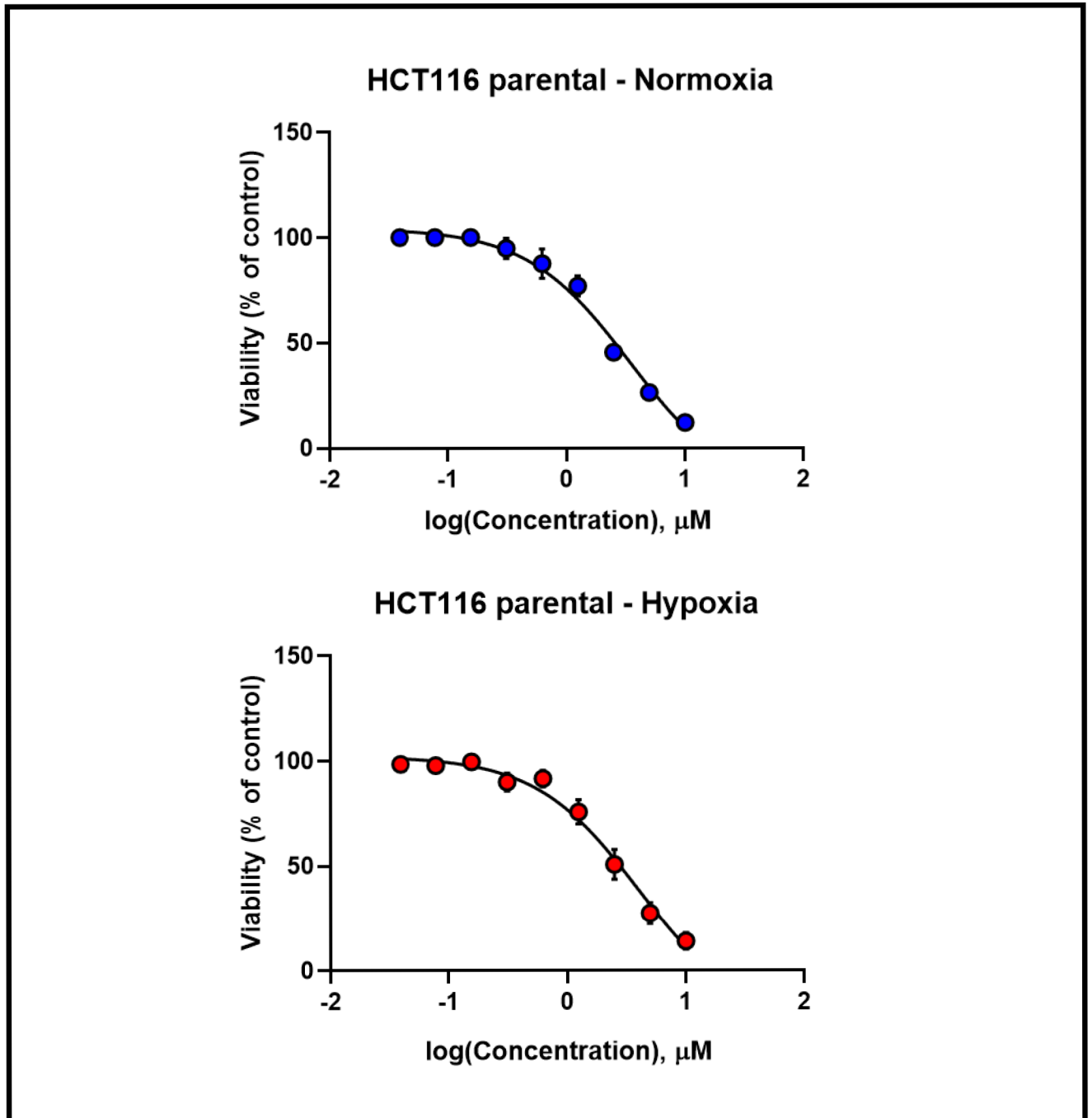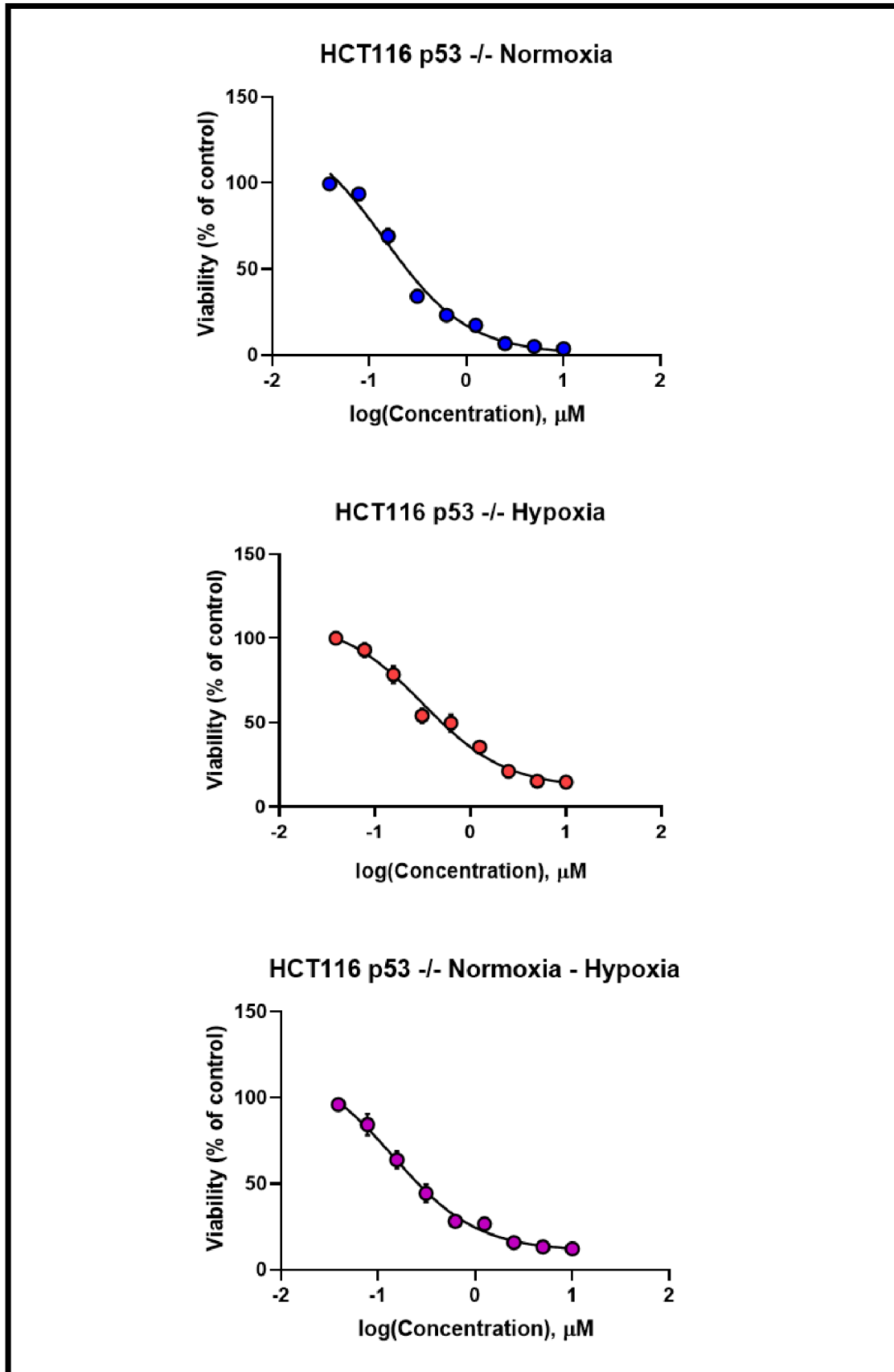
Graph 5.2 – Dose-response curves of YC-1 in HCT116 HIF-1α cells cultured in normoxia and hypoxia. Data are presented as mean ± SEM, n = 4–5.
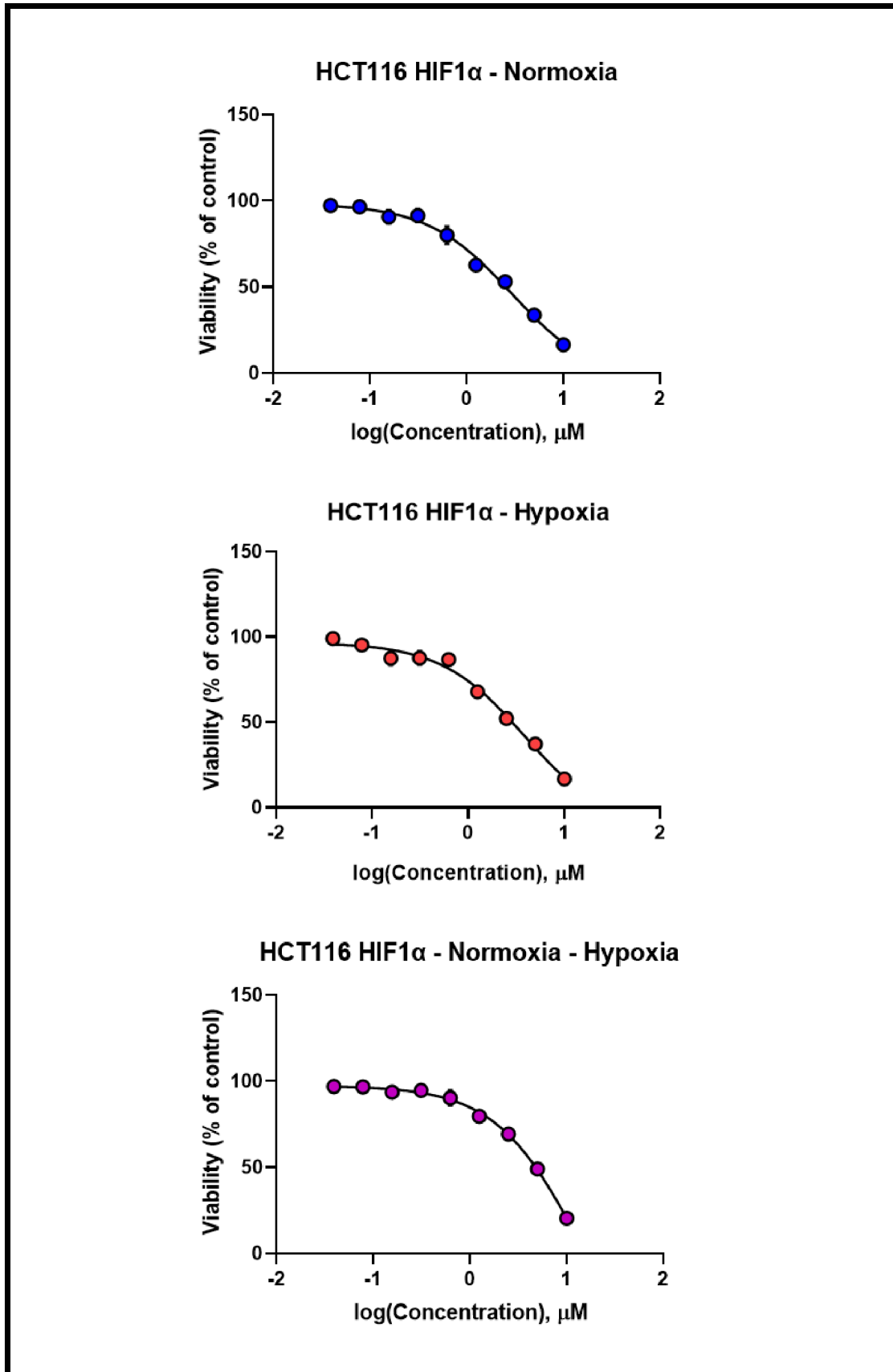
Graph 5.3 – Dose-response curves of Zampanolide in HCT116 parental cells cultured in normoxia and hypoxia. Data are presented as mean ± SEM, n = 2–4

Graph 5.4 – Dose-response curves of Zampanolide in HCT116 p53 -/- cells cultured in normoxia and hypoxia. Data are presented as mean ± SEM, n = 2–3

Graph 5.5 – Dose-response curves of Zampanolide in HCT116 HIF-1α cells cultured in normoxia and hypoxia. Data are presented as mean ± SEM, n = 3–5
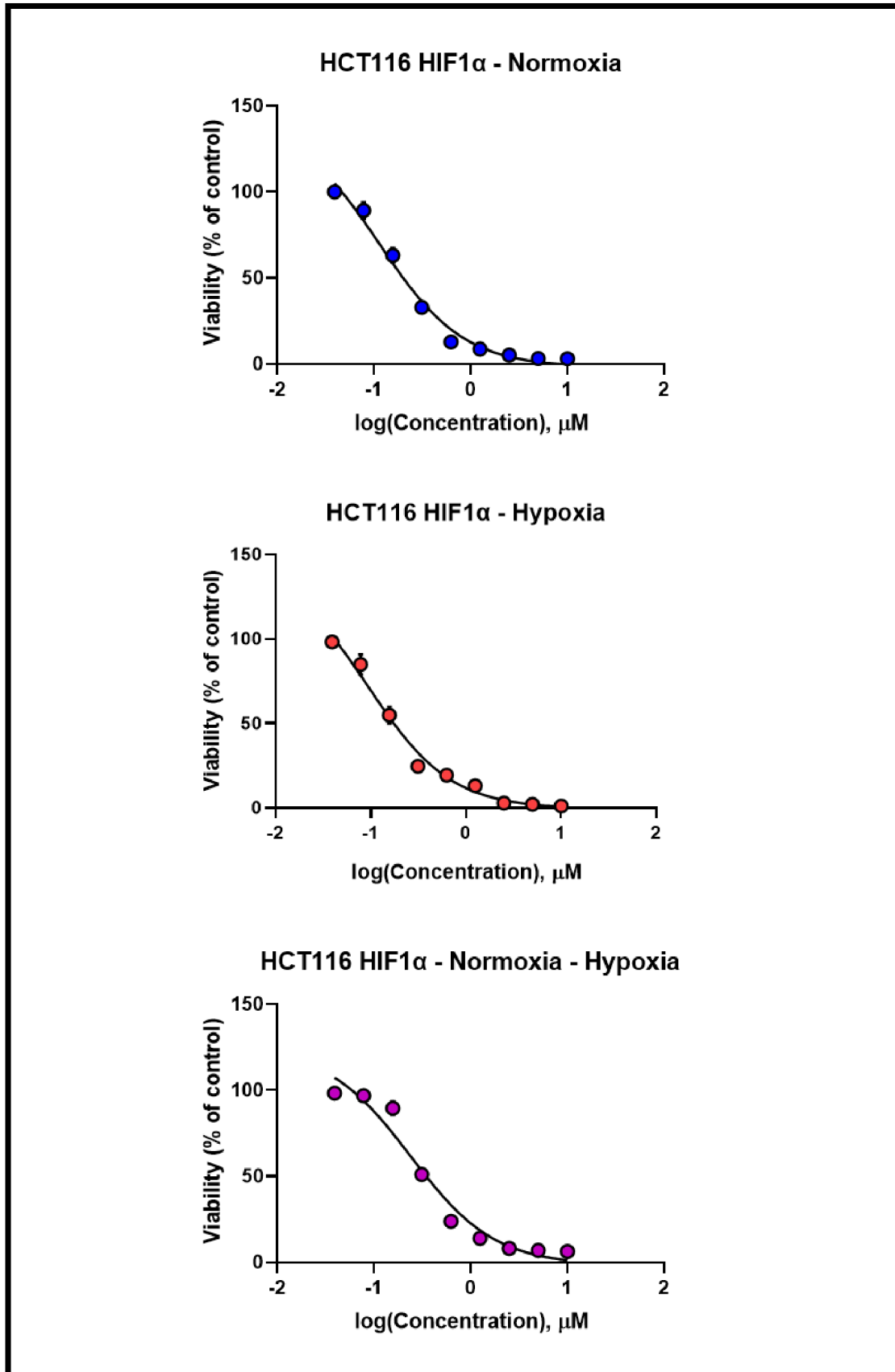
YC-1 treatment induced response only in HCT116 parental and HCT116-HIF-1α cells, and there was no effect of YC-1 on HCT116 p53-/- cells. The IC_{50} of YC-1 in HCT116 parental cells was 3.583 ± 0.6269 µM under Condition 1 and 2.9 ± 0.597 µM in cells cultivated and treated in Condition 2. The IC_{50} of YC-1 in HCT116 parental cells cultured under Condition 3 could not be determined. The IC_{50} value of YC-1 in HCT116 HIF-1α cells under Condition 1 was 2.849 ± 0.3058 µM, Condition 2 was 0.6892 ± 0.1051 µM, and Condition 3 was 0.2793 ± 0.05833 µM. There was no effect of YC-1 on the viability of HCT116 p53 -/- cells.

The IC_{50} value of Zampanolide in HCT116 parental cells was 0.152 ± 0.04037 µM for Condition 1, 0.2755 ± 0.08104 µM for Condition 2, and 0.1096 ± 0.00915 µM for Condition 3. The IC_{50} value of Zampanolide in HCT116 p53-/- cells was 0.1433 ± 0.02701 µM for Condition 1 cells, 0.3834 ± 0.1284 µM for Condition 2 cells, and 0.1392 ± 0.0359 µM for Condition 3 cells. The IC_{50} value of Zampanolide in HCT116-HIF-1α cells was 0.1142 ± 0.01982 µM for Condition 1, 0.146 ± 0.00185 µM for Condition 2, and 0.2426 ± 0.03452 µM for Condition 3.

5.2 Tubulin polymerization assay

Zampanolide is a microtubule-stabilizing agent. Therefore, immunofluorescence and tubulin polymerization assays were used to evaluate its effects on microtubules. Soluble and insoluble protein fractions were isolated from Zampanolide-treated cells cultured under conditions of varying oxygen availability. Proteins were separated by electrophoresis, transferred by Western blotting, and detected by immunolabelling by anti-alpha-tubulin primary antibody and secondary antibody with a fluorescent tag. The percentages of polymerized and depolymerized tubulin were calculated and are shown in Figure 5.1. The representative blots are shown in Figure 5.1.

Figure 5.1 – (A) Representative immunoblots of tubulin soluble (S) and polymerized (P) fractions in HCT116 cell lines treated with Zampanolide in normoxia and hypoxia, n = 2. (B) Quantification of tubulin in soluble and polymerized fractions. Data are presented as mean ± SEM, n = 2.
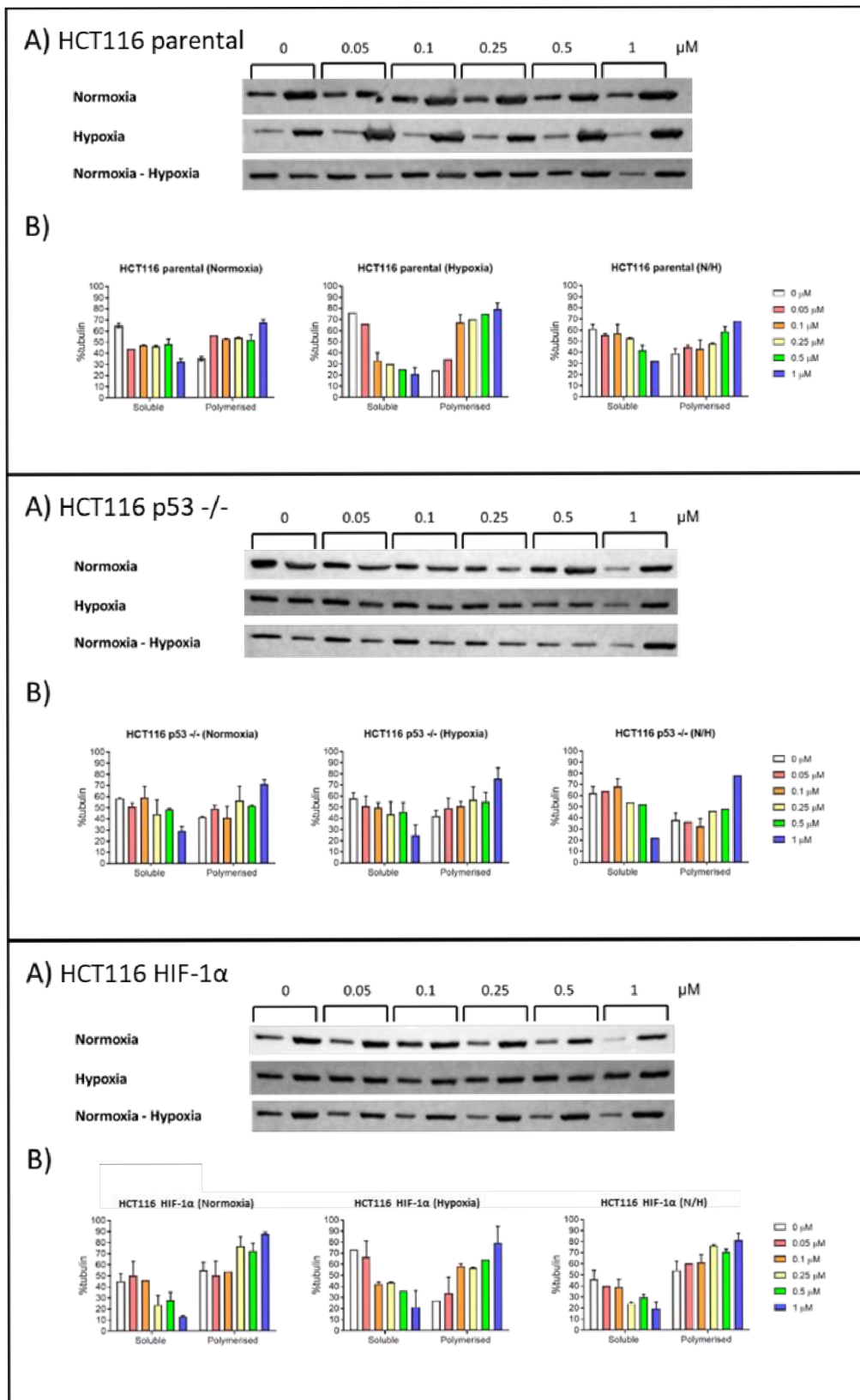
No significant differences were detected in tubulin polymerization in HCT116 parental cells cultivated in Conditions 1 and 3. However, control HCT116 parental cells cultivated in Condition 2 had an increased depolymerized tubulin fraction of over 75 %, compared to control Condition 1 and Condition 3 with depolymerized fraction below 70 %. Also, the polymerized fraction in Condition 2 cells treated with 1 μM Zampanolide exceeded polymerized fractions in Condition 1 and Condition 3 cells at similar concentrations. These results contradict the cell viability assay results because the hypoxic cells had higher IC_{50} values, although their microtubules seem to be the most affected by Zampanolide treatment.

HCT116 p53 -/- cells were evenly affected by Zampanolide treatment under all conditions tested. Compared to HCT116 parental cells in Condition 2, the effects of Zampanolide at concentrations 0.1–1 μM on hypoxic HCT116 p53 -/-were not so profound.

Drug-untreated HCT116 HIF-1α cells in Conditions 1 and 3 had low depolymerized tubulin fractions (45–55 %). However, the drug-untreated HCT116 HIF-1α cells in Condition 2 had depolymerized fraction of around 70 %. The differences between polymerized and depolymerized tubulin fractions were the most profound in HCT116-HIF-1α cells under Condition 2.

5.3 Immunoimaging

Cells were plated on sterilized coverslips and left to attach overnight. The next day, cells were treated with Zampanolide for 1 h in normoxia or hypoxia (Conditions 1 and 3). After the treatment, the cells were fixed with 4% formalin and stained using a primary anti-α-tubulin antibody followed by Alexa Fluour 488 secondary antibody and DAPI nuclear dye. The images obtained from a fluorescent microscope and statistical analysis of microtubule bundling are shown in Figure 5.2.

We observed changes in microtubules in all the tested HCT116-derived cell lines. All treated lineages displayed severe microtubule bundling but only occasional nuclear fragmentation (yellow arrow in a Fig 5.2) or multipolar mitosis (red arrow in a Fig 5.2). Drug-untreated cells also displayed some of the changes that could be interpreted as microtubule bundling or changes in microtubule dynamic, and this type of cell deformity was more prevalent in hypoxic conditions.

Figure 5.2 – (A) Representative images showing changes in microtubules in HCT116 parental cells after Zampanolide treatment in normoxia and hypoxia. n = 3. (B) Quantification of microtubule bundling in cells treated with Zampanolide and control. Data are presented as mean ± SEM, n = 2. Nuclear fragmentation is marked with a yellow arrow and multipolar mitosis is marked with a red arrow.
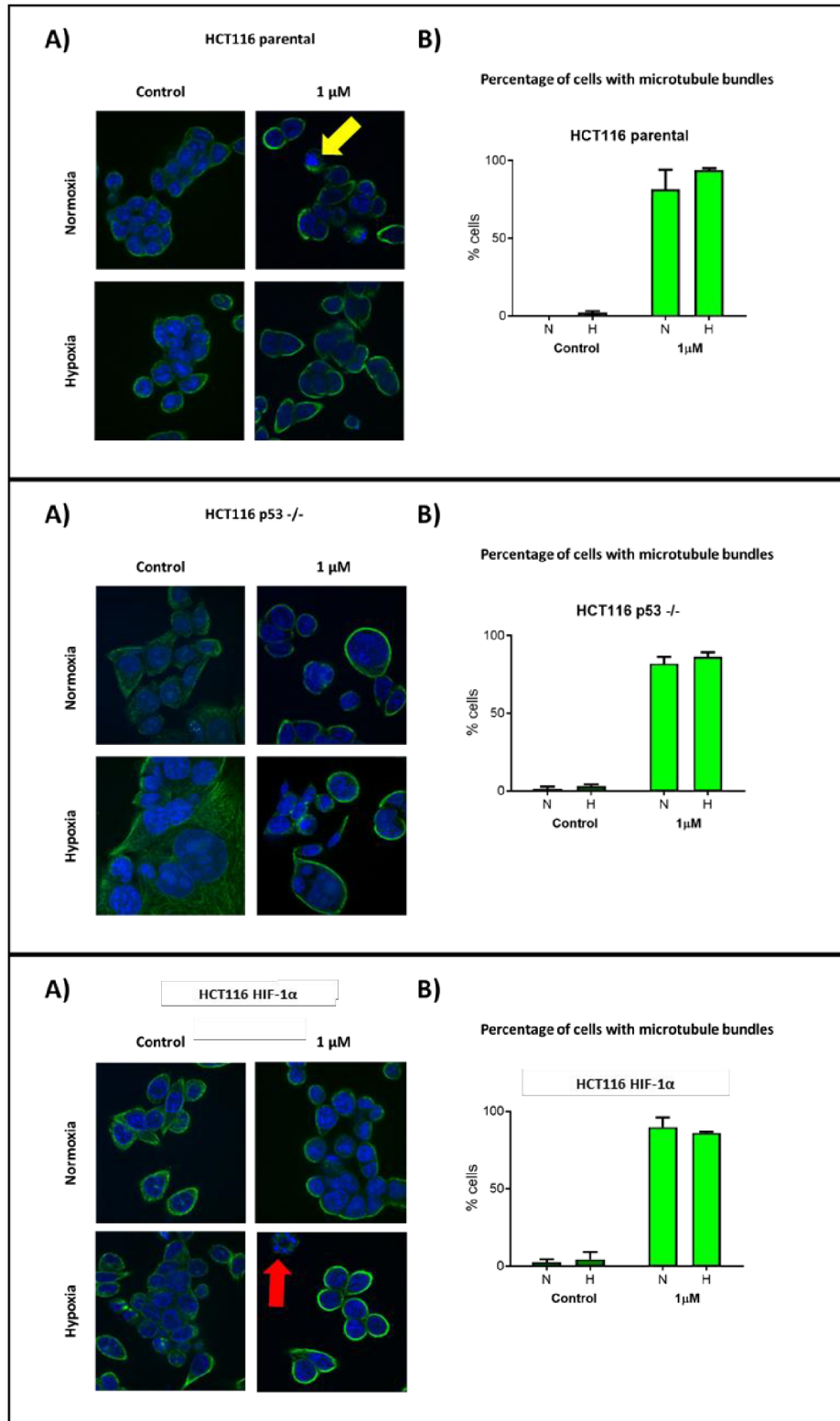
5.4 PARP cleavage

HCT116 Parental and HCT116 p53-/- cells were seeded in 6-well plates and left to attach overnight in hypoxia (Condition 2). The next day they were treated with Zampanolide at $0.1x$ IC_{50}, $0.25x$ $IC_{50,}$ or $1x$ IC_{50} concentrations. Proteins were collected after 3 h, 6h, or 18 h of treatment. Samples were separated by electrophoresis and transferred using Western blotting, and labeled using an anti-PARP primary antibody and a secondary antibody with a fluorescent tag.

The representative blots are shown in Figure 5.3. Calculated percentages of cleaved PARP are also compared in Figure 5.3.

No changes in PARP cleavage were detected in cells treated with Zampanolide in Condition 2 compared to the control or any concentration or time point.

Figure 5.3 – A) Representative immunoblots of PARP in HCT116-derived cell lines treated by Zampanolide in hypoxia with actin loading control, n = 2. (B) Quantification cleaved PARP in samples with various concentrations of Zampanolied treated for 3, 6, or 18 h. Data are presented as mean ± SEM, n = 2.
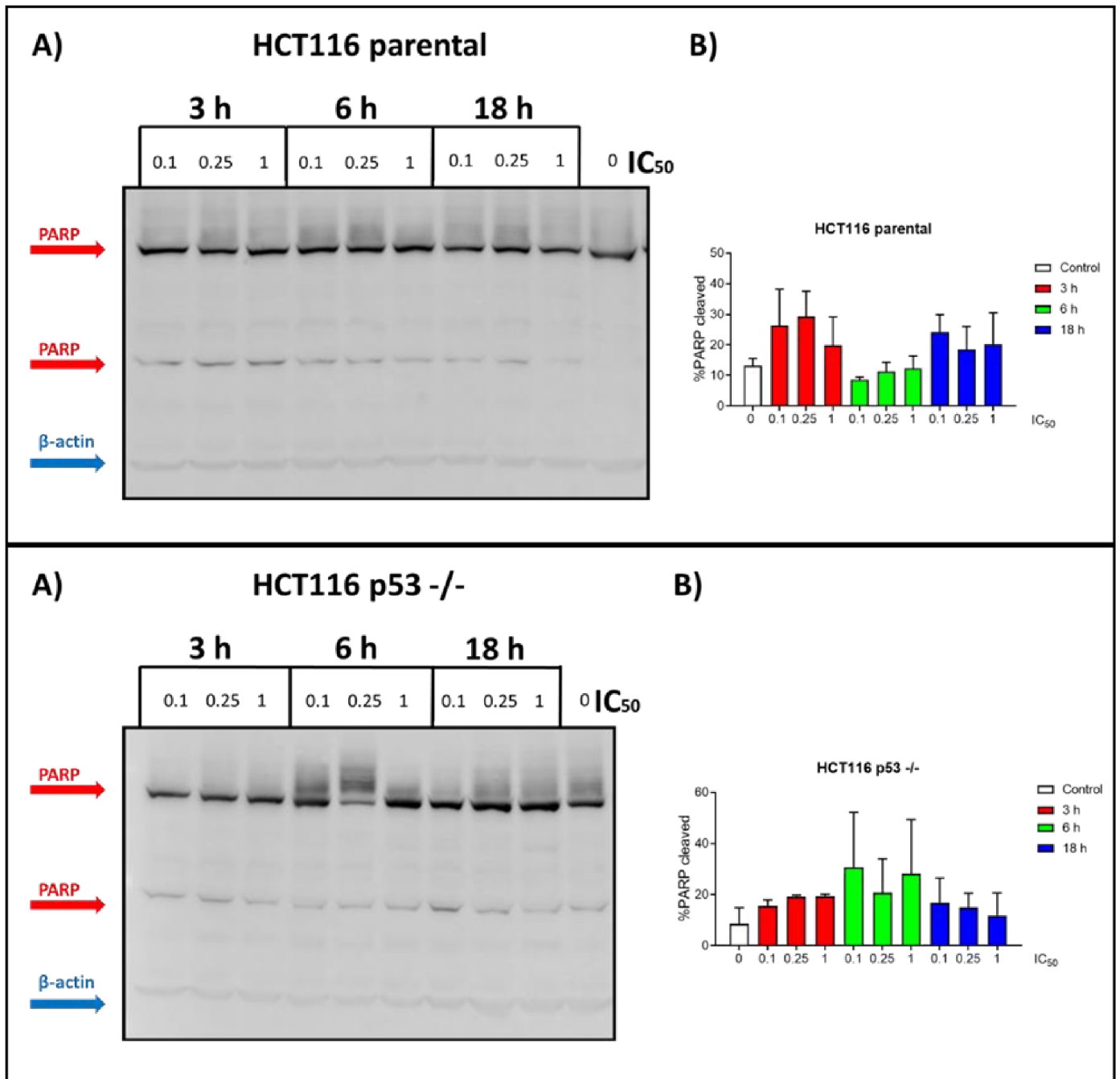
6 DISCUSSION

Stabilization or destabilization of microtubules by MTAs is a common approach in the therapy of solid tumors. However, widely used MTA agents like paclitaxel or vinblastin are susceptible to resistant mechanisms developed by cancer cells. The development of those mechanisms may be enhanced by the hypoxic microenvironment inside solid tumors (Das et al., 2015). Zampanolide is a novel non-taxane MSA with the potential to overcome some of the mechanisms of cancer cell resistance induced by hypoxia (Field et al., 2009).

The effect of Zampanolide on HCT116 cell lines cultivated in hypoxia or normoxia was compared to the cytotoxicity of YC-1, a compound targeting transcription factor HIF-1α involved in the hypoxia signaling pathway (Tsui et al., 2013) (Sun et al., 2007). The cells were treated for 72 h according to protocols described in Chapter 5 RESULTS titled: Conditions 1, 2, or 3, and the cytotoxicity of used compounds was determined using crystal violet staining.

In HCT116116 parental cells, the IC_{50} was higher in Condition 1 and lower in Condition 2. The IC_{50} for Condition 3 could not be accurately determined due to significant differences between replicates. Because Condition 2 cells were cultivated in hypoxia and Condition 1 were not, the IC50 for Condition 2 was expected to be lower since the cells presumably activated hypoxic cell signaling and YC-1 targeted HIF-1α transcription factor.

In HCT116-HIF-1α cells, the differences between IC_{50} values for Conditions 1-3 cells were more significant compared to HCT116 parental cells. Because HCT116 HIF-1α cells presumably overexpress HIF-1α transcription factor, it is understandable that IC_{50} for Condition 2 was at least four times lower than for Condition 1, in which the cells were treated in normoxia and presumably did not overexpress the target protein of YC-1. IC_{50} for Condition 3 was even ten times lower than for Condition 1. To explain this, we may speculate that Condition 2 cells, which were left to attach overnight in a hypoxia incubator, had adjusted their metabolism to hypoxic conditions beforehand, and the effects of treatment on them were not so severe. In contrast, Condition 3 cells entered hypoxia together with treatment and could not conduct hypoxic signaling and adjust to hypoxia.

YC-1 did not affect HCT116 p53 -/- knockout cells. Based on these results, we may suggest that YC-1-induced apoptosis is p53 dependent.

Based on our results, Zampanolide is a more potent drug than YC-1 in normoxic HCT116 cell lines with IC_{50} below 0.2 μM for all the cell lines tested. Also, IC_{50}

of Zampanolide for parental and p53 knockout cells cultivated in Condition 3 was lower than IC_{50} for Condition 1. However, in Condition 2, the IC_{50} values for parental and p53 knockout cells overtly exceeded the IC_{50} values for Condition 1. To explain these unexpected results, we may only speculate that hypoxic preconditioning of Condition 2 cells led to changes induced by hypoxic signalization, which gave those cells an advantage over Condition 3 and even Condition 1. Moreover, in the case of p53 knockout cells, the differences in IC_{50} values between Condition 1 and 3 were so insignificant that they could be considered a statistical error.

In HCT116 HIF-1α cells the IC_{50} values in Conditions 2 and 3 exceeded the IC_{50} value for Condition 1. In these cells, HIF-1α would presumably be overexpressed even in normoxia so the cells are prone to thrive in hypoxic environments.

In order to explain the high resistance of parental and p53 knockout cells to Zampanolide in Condition 2 cells, more experiments would be necessary. Particularly the fact that preexposure to hypoxia may lead to resistance is concerning.

Based on these results, we may conclude that potential HIF-1 overexpression in HCT116 HIF-1α cells may be connected to Zampanolide resistance in hypoxia. The knockout of p53 may have also reduced cell susceptibility to Zampanolide in hypoxia. Moreover, most importantly, the HCT116 cells preconditioned in hypoxia before drug treatment are significantly less susceptible to Zampanolide treatment. All these hypotheses would require more experiments to be proven. For example, repetition of cell viability trial with more replicates and p53 and HIF-1α expression control.

Because Zampanolide is an MSA, tubulin polymerization assays and immunoimaging of microtubules were conducted to evaluate microtubule polymerization. WB was performed with soluble (S) and polymerized (P) tubulin fractions isolated from HCT116 cells treated with increasing concentrations of Zampanolide according to the protocols described in Chapter 5.

Increased tubulin polymerization was detected in all cell lines in all conditions, as expected. In the case of HCT116 parental cells, the changes in percentages of soluble and polymerized tubulin were the fastest in Condition 2. Parental cells in Condition 2 were also the most resistant among parental cells to Zampanolide in the cell viability assay.

In the case of HCT116 p53 knockout cells, the effect of Zampanolide was profound only in the 1 μM concentrations. This could align with the hypothesis that p53 is important for Zampanolide mechanism of action, which could be hindered by p53 mutation.

In the case of HCT116 HIF-1α cells, the changes in polymerized and depolymerized fractions were the most dynamic in Condition 2 varying profoundly between the majority of soluble tubulin fraction in drug-untreated cells and the majority of polymerized fraction in the highest treatment dose.

Overall the microtubule polymerization assay confirms the stabilizing Zampanolide on microtubules; however, it does not say much about the differences in Zampanolide treatment in modified cell lines and various environments. One possible conclusion could be that the microtubule dynamic was only slightly affected in HCT16 p53 knockout cells in treatment concentrations below 1 μM, which could mean that p53 mutation contributes to Zampanolide resistance. To properly investigate these changes, it would be necessary to repeat the experiment with more replicates and maybe a wider range of used drug concentrations.

Microtubules of tested cell lines were also imaged using primary anti-α-tubulin antibody and secondary antibody with fluorescent tag while the nucleus of the cells was visualised using DAPI. All the treated cells displayed severe tubulin bundling, while nuclear fragmentation or multipolar mitosis was rare. Some microtubule structure changes could also be observed in drug-untreated cells, mainly those cultivated in a hypoxic environment. Maybe those changes could be explained by hypoxia-induced stress.

To investigate if Zampanolide activated apoptotic pathways, PARP cleavage was measured using western blotting of isolated complete protein cell lysates from treated HCT116 parental and p53 knockout cells cultivated in hypoxia. However, the replicates prepared varied significantly. So it is impossible to conclude. However, within each replicate, there were no changes between various concentrations. If the PARP cleavage was increased, it was increased evenly in all the treated cells with no regard to the used concentration of Zampanolide or time stamp. There was also PARP cleavage detected repeatedly in drug-untreated cells. The cleavage was probably caused by an unknown common denominator affecting all the cells tested. In conclusion, we could not determine if PARP is cleaved during Zampanolide-induced apoptosis and if there are any differences in PARP cleavage in HCT116 parental and p53 knockout cells.

7 CONCLUSION

The aim of this thesis was to determine the effects of Zampanolide on human colorectal carcinoma cell line HCT116 in hypoxic and normoxic conditions. To compare Zampanolide effects to HIF-1α targeting YC-1 and to investigate the role of p53 and HIF-1α in cell's response to Zampanolide in normoxia and hypoxia.

We conclude that Zampanolide is effective in 500–100 nM ranges in HCT116 cells. However, p53 knockout and HIF-1α overexpression may contribute to hypoxia-induced resistance to Zampanolide. Also, HCT116 cells preconditioned in hypoxia prior Zampanolide treatment may display Zampanolide resistance.

Zampanolide causes severe microtubule bundling in treated cells in normoxia and hypoxia, effectively hindering mitosis and cellular transport. Zampanolide-induced polymerization of tubulin may be slightly reduced by p53 knockout.

It remains unclear whether Zampanolide-induced cell death is carried out through PARP-cleavage.

Overall the mechanism by which the cells evade the Zampanolide-induced apoptosis due to hypoxia is unknown and unexpected. Although we may speculate that HIF-1α is involved since HCT116 HIF-1α cells displayed increased resistance to Zampanolide treatment compared to cells without this modification.

The resistance of hypoxia preconditioned cells to Zampanolide is concerning since hypoxic cells inside solid tumors are starved of oxygen because of imperfect neovascularization and critical tumor diameter, which is a state that precedes treatment.

Based on the results in this thesis, Zampanolide potential as a drug that can overcome hypoxia-induced resistance is scarce. However, further experiments are needed to confirm this hypothesis, and cell resistance mechanisms to Zampanolide must be evaluated in detail. The imperfections of the trial conduction may also have contributed to unexpected results.

8 REFERENCES

ALBERTS, Bruce. *Molecular biology of the cell*. 5th ed. New York: Garland Science, c2008. ISBN 978-0-8153-4105-5.

AMARGANT, Farners, Montserrat BARRAGAN, Rita VASSENA a Isabelle VERNOS. Insights of the tubulin code in gametes and embryos: from basic research to potential clinical applications in humans†. *Biology of Reproduction* [online]. 2019, **100**(3), 575-589 [cit. 2022-12-20]. ISSN 0006-3363. DOI:10.1093/biolre/ioy203

World Health Organization (WHO) [online]. Cancer, Copyright © [cit. 22.12.2022]. https://www.who.int/news-room/fact-sheets/detail/cancer

CHEN, Qiao-Hong a David G. I. KINGSTON. Zampanolide and dactylolide: cytotoxic tubulin-assembly agents and promising anticancer leads. *Nat. Prod. Rep* [online]. 2014, **31**(9), 1202-1226 [cit. 2022-12-22]. ISSN 0265-0568. DOI:10.1039/C4NP00024B

CHEN, Guanglin, Ziran JIANG, Qiang ZHANG, Guangdi WANG a Qiao-Hong CHEN. New Zampanolide Mimics: Design, Synthesis, and Antiproliferative Evaluation. *Molecules* [online]. 2020, **25**(2) [cit. 2021-10-26]. ISSN 1420-3049. DOI:10.3390/molecules25020362

COMERFORD KM, Wallace TJ, Karhausen J, Louis NA, Montalto MC, Colgan SP. Hypoxia-inducible factor-1-dependent regulation of the multidrug resistance (MDR1) gene. Cancer Res. 2002 Jun 15;62(12):3387-94. PMID: 12067980.

COOPER, Geoffrey M. *The Cell: A Molecular Approach. 2nd Edition:* Sinauer Associates, 2000

DALBETH, Nicola, Thomas J. LAUTERIO a Henry R. WOLFE. Mechanism of Action of Colchicine in the Treatment of Gout. Clinical Therapeutics [online]. 2014, 36(10), 1465-1479 [cit. 2023-02-04]. ISSN 01492918. DOI:10.1016/j.clinthera.2014.07.017

DAS, Viswanath, Jana ŠTĚPÁNKOVÁ, Marián HAJDÚCH a John H. MILLER. Role of tumor hypoxia in acquisition of resistance to microtubule-stabilizing drugs. *Biochimica et Biophysica Acta (BBA) - Reviews on Cancer* [online]. 2015, **1855**(2), 172-182 [cit. 2021-10-26]. ISSN 0304419X. DOI:10.1016/j.bbcan.2015.02.001

DONEHOWER, Lawrence A., Michele HARVEY, Betty L. SLAGLE, Mark J. MCARTHUR, Charles A. MONTGOMERY, Janet S. BUTEL a Allan BRADLEY. Mice deficient for p53 are developmentally normal but susceptible to spontaneous tumours. *Nature* [online]. 1992, **356**(6366), 215-221 [cit. 2022-12-29]. ISSN 0028-0836. DOI:10.1038/356215a0

FIELD, Jessica, Peter NORTHCOTE, Ian PATERSON, Karl-Heinz ALTMANN, J. DÍAZ a John MILLER. Zampanolide, a Microtubule-Stabilizing Agent, Is Active in Resistant Cancer Cells and Inhibits Cell Migration. *International Journal of Molecular Sciences* [online]. 2017, **18**(5) [cit. 2021-10-26]. ISSN 1422-0067. DOI:10.3390/ijms18050971

FIELD, Jessica J., A. Jonathan SINGH, Arun KANAKKANTHARA, Tu'ikolongahau HALAFIHI, Peter T. NORTHCOTE a John H. MILLER. Microtubule-Stabilizing Activity of Zampanolide, a Potent Macrolide Isolated from the Tongan Marine Sponge Cacospongia mycofijiensis. Journal of Medicinal Chemistry [online]. 2009, 52(22), 7328-7332 [cit. 2023-02-01]. ISSN 0022-2623. DOI: 10.1021/jm901249g

HALAFIHI, Peter T. NORTHCOTE a John H. MILLER. Microtubule-Stabilizing Activity of Zampanolide, a Potent Macrolide Isolated from the Tongan Marine Sponge Cacospongia mycofijiensis. *Journal of Medicinal Chemistry* [online]. 2009, **52**(22), 7328-7332 [cit. 2022-12-22]. ISSN 0022-2623. DOI:10.1021/jm901249g

FONG, Guo-Hua, Janet ROSSANT, Marina GERTSENSTEIN a Martin L. BREITMAN. Role of the Flt-1 receptor tyrosine kinase in regulating the assembly of vascular endothelium. *Nature* [online]. 1995, **376**(6535), 66-70 [cit. 2022-12-19]. ISSN 0028-0836. DOI:10.1038/376066a0

GHOSH, Arun K. a Xu CHENG. Enantioselective Total Synthesis of (−)-Zampanolide, a Potent Microtubule-Stabilizing Agent. *Organic Letters* [online]. 2011, **13**(15), 4108-4111 [cit. 2021-10-26]. ISSN 1523-7060. DOI:10.1021/ol201626h

GOTTESMAN, Michael M., Tito FOJO a Susan E. BATES. Multidrug resistance in cancer: role of ATP–dependent transporters. *Nature Reviews Cancer* [online]. 2002, **2**(1), 48-58 [cit. 2022-12-19]. ISSN 1474-175X. DOI:10.1038/nrc706

HU, Tao, Zhen LI, Chun-Ying GAO a Chi Hin CHO. Mechanisms of drug resistance in colon cancer and its therapeutic strategies. *World Journal of Gastroenterology* [online]. 2016, **22**(30) [cit. 2022-12-22]. ISSN 1007-9327. DOI:10.3748/wjg.v22.i30.6876

JOHNSON, T. A., Tenney, K., Cichewicz, R. H., Morinaka, B. I., White, K. N., Amagata, T., ... & Crews, P. (2007). Sponge-derived fijianolide polyketide class: further evaluation of their structural and cytotoxicity properties. Journal of medicinal chemistry, 50(16), 3795-3803.

JORDAN, Mary Ann a Leslie WILSON. Microtubules as a target for anticancer drugs. *Nature Reviews Cancer* [online]. 2004, **4**(4), 253-265 [cit. 2022-12-20]. ISSN 1474-175X. DOI:10.1038/nrc1317

KAVALLARIS, Maria. Microtubules and resistance to tubulin-binding agents. *Nature Reviews Cancer* [online]. 2010, **10**(3), 194-204 [cit. 2022-12-23]. ISSN 1474-175X. DOI:10.1038/nrc2803

KESAVARDHANA, Sannula, R.K. Subbarao MALIREDDI a Thirumala-Devi KANNEGANTI. Caspases in Cell Death, Inflammation, and Pyroptosis. *Annual Review of Immunology* [online]. 2020, **38**(1), 567-595 [cit. 2022-12-30]. ISSN 0732-0582. DOI:10.1146/annurev-immunol-073119-095439

KIM, Ryungsa. Unknotting the roles of Bcl-2 and Bcl-xL in cell death. *Biochemical and Biophysical Research Communications* [online]. 2005, **333**(2), 336-343 [cit. 2022-12-21]. ISSN 0006291X. DOI:10.1016/j.bbrc.2005.04.161

LEE, Pearl, Navdeep S. CHANDEL a M. Celeste SIMON. Cellular adaptation to hypoxia through hypoxia inducible factors and beyond. *Nature Reviews Molecular Cell Biology* [online]. 2020, **21**(5), 268-283 [cit. 2022-11-11]. ISSN 1471-0072. DOI:10.1038/s41580-020-0227-y

LIEBL, Magdalena C. a Thomas G. HOFMANN. The Role of p53 Signaling in Colorectal Cancer. *Cancers* [online]. 2021, **13**(9) [cit. 2022-12-29]. ISSN 2072-6694. DOI:10.3390/cancers13092125

LIU J, Towle MJ, Cheng H, Saxton P, Reardon C, Wu J, Murphy EA, Kuznetsov G, Johannes CW, Tremblay MR, Zhao H, Pesant M, Fang FG, Vermeulen MW, Gallagher BM Jr, Littlefield BA. In vitro and in vivo anticancer activities of synthetic (-)-laulimalide, a marine natural product microtubule stabilizing agent. Anticancer Res. 2007 May-Jun;27(3B):1509-18. PMID: 17595769

LU, Yan, Jianjun CHEN, Min XIAO, Wei LI a Duane D. MILLER. An Overview of Tubulin Inhibitors That Interact with the Colchicine Binding Site. Pharmaceutical Research [online]. 2012, 29(11), 2943-2971 [cit. 2023-02-01]. ISSN 0724-8741. DOI:10.1007/s11095-012-0828-z

LYONS, Timothy W., Christopher T. REINHARD a Noah J. PLANAVSKY. The rise of oxygen in Earth's early ocean and atmosphere. *Nature* [online]. 2014, **506**(7488), 307-315 [cit. 2022-11-11]. ISSN 0028-0836. DOI:10.1038/nature13068

MALEKAN, Mohammad, Mohammad Ali EBRAHIMZADEH a Fateme SHEIDA. The role of Hypoxia-Inducible Factor-1alpha and its signaling in melanoma. *Biomedicine & Pharmacotherapy* [online]. 2021, **141** [cit. 2022-12-23]. ISSN 07533322. DOI:10.1016/j.biopha.2021.111873

MEEK, David W. The p53 response to DNA damage. *DNA Repair* [online]. 2004, **3**(8-9), 1049-1056 [cit. 2022-12-29]. ISSN 15687864. DOI:10.1016/j.dnarep.2004.03.027

MILLS, C.N., Joshi, S.S. & Niles, R.M. Expression and function of hypoxia inducible factor-1 alpha in human melanoma under non-hypoxic conditions. *Mol Cancer* **8**, 104 (2009). DOI: 10.1186/1476-4598-8-104

MOUDI M, Go R, Yien CY, Nazre M. Vinca alkaloids. Int J Prev Med. 2013 Nov;4(11):1231-5. PMID: 24404355; PMCID: PMC3883245.

NEGI, Arvind S., Yashveer GAUTAM, Sarfaraz ALAM, Debabrata CHANDA, Suaib LUQMAN, Jayanta SARKAR, Feroz KHAN a Rituraj KONWAR. Natural antitubulin agents: Importance of 3,4,5-trimethoxyphenyl fragment. Bioorganic & Medicinal Chemistry [online]. 2015, 23(3), 373-389 [cit. 2023-01-30]. ISSN 09680896. DOI: doi:10.1016/j.bmc.2014.12.027

OBACZ, Joanna, Silvia PASTOREKOVA, Borek VOJTESEK a Roman HRSTKA. Cross-talk between HIF and p53 as mediators of molecular responses to physiological and genotoxic stresses. *Molecular Cancer* [online]. 2013, **12**(1) [cit. 2022-12-30]. ISSN 1476-4598. DOI:10.1186/1476-4598-12-93

PENG, Wan-Xin, Fei-Yan PAN, Xiao-Jin LIU, Shen NING, Na XU, Fan-Li MENG, Yi-Qian WANG a Chao-Jun LI. Hypoxia Stabilizes Microtubule Networks and Decreases Tumor Cell Chemosensitivity to Anticancer Drugs Through Egr-1. *The Anatomical Record: Advances in Integrative Anatomy and Evolutionary Biology* [online]. 2010, **293**(3), 414-420 [cit. 2022-12-28]. ISSN 19328486. DOI:10.1002/ar.21086

PERONNE, Lauralie, Eric DENARIER, Ankit RAI, et al. Two Antagonistic Microtubule Targeting Drugs Act Synergistically to Kill Cancer Cells. *Cancers* [online]. 2020, **12**(8) [cit. 2021-10-26]. ISSN 2072-6694. DOI:10.3390/cancers12082196

RASPAGLIO, Giuseppina, Flavia FILIPPETTI, Silvia PRISLEI, et al. Hypoxia induces class III beta-tubulin gene expression by HIF-1α binding to its 3' flanking region. *Gene* [online]. 2008, **409**(1-2), 100-108 [cit. 2022-12-23]. ISSN 03781119. DOI:10.1016/j.gene.2007.11.015

ŘEHULKA, Jiří, Narendran ANNADURAI, Ivo FRYDRYCH, et al. Cellular effects of the microtubule-targeting agent peloruside A in hypoxia-conditioned colorectal carcinoma cells. *Biochimica et Biophysica Acta (BBA) - General Subjects* [online]. 2017, **1861**(7), 1833-1843 [cit. 2021-10-26]. ISSN 03044165. DOI:10.1016/j.bbagen.2017.03.023

ŘEHULKA, Jiří, Narendran ANNADURAI, Ivo FRYDRYCH, Petr DŽUBÁK, John H. MILLER, Marián HAJDÚCH a Viswanath DAS. Peloruside A-Induced Cell Death in Hypoxia Is p53 Dependent in HCT116 Colorectal Cancer Cells. *Journal of Natural Products* [online]. 2018, **81**(3), 634-640 [cit. 2021-10-26]. ISSN 0163-3864. DOI:10.1021/acs.jnatprod.7b00961

RISINGER, April L., Francis J. GILES a Susan L. MOOBERRY. Microtubule dynamics as a target in oncology. Cancer Treatment Reviews [online]. 2009, 35(3), 255-261 [cit. 2023-01-30]. ISSN 03057372. Dostupné z: doi:10.1016/j.ctrv.2008.11.001

SEMENZA GL, Roth PH, Fang HM & Wang GL (1994). Transcriptional regulation of genes encoding glycolytic enzymes by hypoxia-inducible factor 1. J Biol Chem 269, 23757–23763

SHERR, Charles J a Jason D WEBER. The ARF/p53 pathway. *Current Opinion in Genetics & Development* [online]. 2000, **10**(1), 94-99 [cit. 2022-12-29]. ISSN 0959437X. DOI:10.1016/S0959-437X(99)00038-6

SHIBUYA, M. Vascular Endothelial Growth Factor (VEGF) and Its Receptor (VEGFR) Signaling in Angiogenesis: A Crucial Target for Anti- and Pro-Angiogenic Therapies. *Genes & Cancer* [online]. 2012, **2**(12), 1097-1105 [cit. 2022-12-19]. ISSN 1947-6019. DOI:10.1177/1947601911423031

STUKALIN, Igor, Nimira ALIMOHAMED a Daniel Y.C. HENG. Contemporary treatment of metastatic renal cell carcinoma. *Oncology Reviews* [online]. 2016 [cit. 2022-12-19]. ISSN 1970-5565. DOI:10.4081/oncol.2016.295

SUNG, Hyuna, Jacques FERLAY, Rebecca L. SIEGEL, Mathieu LAVERSANNE, Isabelle SOERJOMATARAM, Ahmedin JEMAL a Freddie BRAY. Global Cancer Statistics 2020: GLOBOCAN Estimates of Incidence and Mortality Worldwide for 36 Cancers in 185 Countries. *CA: A Cancer Journal for Clinicians* [online]. 2021, **71**(3), 209-249 [cit. 2022-12-22]. ISSN 0007-9235. DOI:10.3322/caac.21660

SUN, H-L, Y-N LIU, Y-T HUANG, et al. YC-1 inhibits HIF-1 expression in prostate cancer cells: contribution of Akt/NF-κB signaling to HIF-1α accumulation during hypoxia. *Oncogene* [online]. 2007, **26**(27), 3941-3951 [cit. 2022-12-19]. ISSN 0950-9232. DOI:10.1038/sj.onc.1210169

SUZUKI, Hiroyuki, Akihiro TOMIDA a Takashi TSURUO. Dephosphorylated hypoxia-inducible factor 1α as a mediator of p53-dependent apoptosis during hypoxia. *Oncogene* [online]. 2001, **20**(41), 5779-5788 [cit. 2022-12-30]. ISSN 0950-9232. DOI:10.1038/sj.onc.1204742

TSUI L, Fong TH, Wang IJ. The effect of 3-(5'-hydroxymethyl-2'-furyl)-1-benzylindazole (YC-1) on cell viability under hypoxia. Mol Vis. 2013 Nov 16;19:2260-73. PMID: 24265542; PMCID: PMC3834593.

VU, Ha Linh a Andrew E. APLIN. Targeting mutant NRAS signaling pathways in melanoma. *Pharmacological Research* [online]. 2016, **107**, 111-116 [cit. 2022-12-22]. ISSN 10436618. DOI:10.1016/j.phrs.2016.03.007

WU, Yan, Andrea T. HOOPER, Zhaojing ZHONG, Larry WITTE, Peter BOHLEN, Shahin RAFII a Daniel J. HICKLIN. The vascular endothelial growth factor receptor (VEGFR-1) supports growth and survival of human breast carcinoma. *International Journal of*

YU, Jingwei, Jing GAO, Zhihao LU, et al. Combination of microtubule associated protein-tau and β-tubulin III predicts chemosensitivity of paclitaxel in patients with advanced gastric cancer. *European Journal of Cancer* [online]. 2014, **50**(13), 2328-2335 [cit. 2022-12-27]. ISSN 09598049. DOI:10.1016/j.ejca.2014.06.017

ZHANG, Zhen, Li YAO, Jinhua YANG, Zhenkang WANG a Gang DU. PI3K/Akt and HIF-1 signaling pathway in hypoxia-ischemia (Review). *Molecular Medicine Reports* [online]. 2018 [cit. 2022-12-22]. ISSN 1791-2997. DOI:10.3892/mmr.2018.9375